Since January 2020 Elsevier has created a COVID-19 resource centre with free information in English and Mandarin on the novel coronavirus COVID-19. The COVID-19 resource centre is hosted on Elsevier Connect, the company's public news and information website.

Sensing and Bio-Sensing Research 30 (2020) 100382

Contents lists available at ScienceDirect

Sensing and Bio-Sensing Research

journal homepage: www.elsevier.com/locate/sbsr

Review: Applications of surface-enhanced fluorescence (SEF) spectroscopy in bio-detection and biosensing

Alisher Sultangaziyev, Rostislav Bukasov *

Chemistry Department, SSH, Nazarbayev University, Nur-Sultan 010000, Kazakhstan

ARTICLE INFO

Keywords:
Surface-enhanced fluorescence
Metal-enhanced fluorescence
Biosensing
Bio-detection
Limit of detection
Enhancement factor

ABSTRACT

Surface-enhanced fluorescence (SEF) is rapidly becoming one of the main spectroscopic techniques for the detection of a variety of biomolecules and biomarkers. The main reasons for this trend are the high sensitivity and selectivity, robustness, and speed of this analytical method. Each year, the number of applications that utilize this phenomenon increases and with each such work, the complexity and novelty of the used substrates, procedures, and analytes rises. To obtain a clearer view of this phenomenon and research area, we decided to combine 76 valuable research articles from a variety of different research groups into this mini-review. We present and describe these works concisely and clearly, with a particular interest in the quantitative parameters of the experiment. These sources are classified according to the nature of the analyte, on the contrary to most reviews, which sort them by substrate nature. This point of view gives us insight into the development of this research area and the consequent increase in the complexity of the analyte nature. Moreover, this type of sorting can show possible future routes for the expansion of this research area. Along with the analytes, we can also pay attention to the substrates used for each situation and how the development of substrates affects the direction of research and subsequently, the choice of an analyte. About 108 sources and several interesting trends in the SEF research area over the past 25 years are discussed in this mini-review.

1. Introduction

Over the past 30 years, the phenomenon of fluorescence has become an irreplaceable analytical tool in biotechnology and medicine. Fluorescence provides fast and reliable detection of molecules with picogram sensitivity, but further development of this technique in terms of sensitivity is still highly desirable [1]. This property of fluorescence is usually limited by the quantum yield and fluorescence lifetime. The quantum yield (Q_0) determines the efficiency of the fluorescence and demonstrates the ratio of photon emission against non-radiative decay:

$$Q_0 = \frac{\Gamma}{\Gamma + k_{nr} + k_q} \quad (1)$$

where Γ is the radiative decay rate of the fluorophore, which is the rate of photon emission. The terms k_{nr} and k_q depict the phenomena by which the fluorophore can return to the ground state: non-radiative decay and other quenching processes, respectively. The fluorescence lifetime is described by the time for which the fluorophore remains in the first singlet state on the Jablonski diagram [2], and is illustrated by the following equation:

$$\tau_0 = \frac{1}{\Gamma + k_{nr} + k_q} \quad (2)$$

Usually, these parameters can be altered by changing the magnitude of non-radiative decay and other quenching processes, as the radiative decay rate Γ is a constant value which depends on the extinction coefficient of the fluorophore [3]. However, by placing the fluorophore near a conducting metal surface or particle, it is possible to change the radiative decay rate Γ and influence the quantum yield and fluorescence lifetime [4].

The theoretical background behind the effects of metal surfaces on fluorescence has been well studied and summarized in various articles and reviews [5–7]. It was found that two main effects are responsible for the change in fluorescence in the proximity of a metal surface. The first effect, called the "lightning rod effect" [8], is the amplification of incident light by the inner free electrons of the metal. This effect can be utilized to obtain localized enhancement of fluorescence and to significantly increase the rate of excitation and intensity. The second effect is

* Corresponding author.
E-mail address: rostislav.bukasov@nfu.edu.kz (R. Bukasov).

https://doi.org/10.1016/j.sbsr.2020.100382
Received 6 July 2020; Received in revised form 9 October 2020; Accepted 14 October 2020
Available online 16 October 2020

the increase in radiative decay rate through an additional metal-induced radiative rate Γ_m. This term modifies eqs. 1 and 2 accordingly:

$$Q_m = \frac{\Gamma + \Gamma_m}{\Gamma + \Gamma_m + k_{nr} + k_q} \quad (3)$$

$$\tau_m = \frac{1}{\Gamma + \Gamma_m + k_{nr} + k_q} \quad (4)$$

Thus, an increase in quantum yield and a decrease in fluorescence lifetime can be achieved by placing the fluorophore near a conducting metal surface or particle. The combination of these phenomena is called metal-enhanced fluorescence (MEF) or more broadly, surface-enhanced fluorescence (SEF) [9].

This effect was first observed and discovered in the late 1960s by Drexhage, during his investigations on the lifetime of fluorescence in the presence of metal film [10,11]. In the next several decades this topic gained more attention, mostly due to substantial research works by the group of Lakowicz and Geddes [12–15]. The most popular substrate of choice at that time was silver island films (SiFs) [16–18]. Later, the potential use of nanoparticles was revealed (especially silver, gold, and core-shell nanoparticles) [19–21]. Nowadays, the use of quantum dots and biochips for SEF is becoming increasingly popular [22–24]. Consequently, with the development of new metallic surfaces and nanostructures, the range of possible MEF applications has expanded [25].

Despite this considerable development, we could not find a reasonable number of comprehensive reviews concerning the analytical side of this subject. Nonetheless, we should mention the classic works of the Lakowicz and Geddes group in the early 2000s and the reviews of recent years that have contributed to this field [12,26,27]. In particular, the group of Dr. Xie published a thorough study on the applications of MEF in biotechnology and its increasing potential using computational modeling and novel fabrication techniques [28]. Also recently, the group of Dr. Koh was able to showcase the promising applications of MEF in state-of-the-art biosensing, and discussed the future of this biodetection method in their respective review [29]. However, these reviews are more concentrated on the nature of SEF substrates, their preparation, properties, and applications; a handful of reviews take on more of a theoretical approach [25,30–33]. Therefore, we decided to write a review that systematically describes applications of SEF in biosensing through major analytical parameters, such as limit of detection (LOD), enhancement factor (EF), etc. We will start our review from the simplest metal ions and small organic molecules, gradually increasing the level of complexity up to toxins and bacteria, and finally we will discuss several prominent trends across these studies.

2. Metal ions

With the first development of fluorescence spectroscopy, research on the detection of metal ions sprouted readily, as it is of foremost importance to analyze our environment for highly toxic metals like mercury, lead, etc. This was also the case for MEF, as several research papers were published on this topic in the past two decades. All these papers report on the development of novel sensors for the selective and sensitive detection of metal ions.

The first major example of applying SEF for the detection of metal ions was presented by the group of Dr. Perish Chandra Ray in 2007, where they used a battery-operated ultrasensitive gold nanoparticle-based nanomaterial surface energy transfer probe for the detection of Hg^{2+} ions in soil, water, and fish [34]. They reported a detection limit of 2 ppt in the range of 0.8–170 ppb. Moreover, the selectivity assessment shows the exact preference of this sensor for the detection of Hg^{2+} ions against 12 other metal ions. This successful presentation of fluorescence capabilities for the detection of metal ions, paved the way for new research in this area in the 2010s.

In 2014, two different research groups, led by Dr. Yu and Dr. Li, presented the detection of Hg^{2+} ions with 1.4 nM and 1 nM limits of detection, respectively [35,36]. The group of Dr. Yu used silver-silica core-shell nanoparticles modified with DNA strands for the detection of Hg^{2+} ions in the range between 0 and 100 nM. They also showed sensitive detection of silver ions with a limit of detection of 20 nM.

In the following years, the group of Dr. Zhang developed a silver nanocube fluorescent nanocomposite for the detection of Cu^{2+} ions [37]. This silver nanocube was functionalized with a silica interlayer and a mesoporous organosilica outer layer. This nanocomposite showed 3-fold fluorescence enhancement and an LOD for Cu^{2+} of 0.3 μM, with a linear range of 1–5 μM. Dr. Zhang's group also performed a selectivity experiment, which showed the high selectivity for Cu^{2+} ions as compared to 14 other heavy metals. The group of Dr. Li, on the other hand, used a simpler nanostructure, composed of silver nanoparticles functionalized with thiol-DNA [38]. Using this sensor, they achieved sensitive detection of Hg^{2+} ions in the range between 1 and 80 nM. In the following years, the group of Dr. Yan showcased the detection of lead ions using $ZnFe_2O_4$@Au-Ag bifunctional nanocomposite and DNA/CeO2 complex. They achieved a 0.3 pM detection limit with a concentration range of 1 pM – 3 μM. Furthermore, they showed that this biosensor can be readily recycled using Cy3-17DS-CeO_2 in three cycles.

Among these studies, the highest fluorescence enhancement was presented by Darbha et al. for the detection of mercury (II) ions by using a gold nanoparticle-based probe [34]. Moreover, they were able to assess the mercury concentration not only in water but in soil and fish as well, with an LOD of 2 ppt. This excellent result was possible by utilizing a surface energy transfer between a gold nanoparticle and organic dye. This interaction can easily be quenched in the presence of heavy metal ions (mercury, in this case). The same level of sensitivity was shown by Liang et al., with a 0.3 pM limit of detection for Pb^{2+} ions [38]. However, this method is only applicable for the detection of lead in water samples. Nevertheless, this sensor – based on ZnFe2O4@Au-Ag bifunctional nanocomposite – can be recycled. Overall, both methods show the successful use of MEF in the detection of heavy metal ions. However, the synthesis of these sensors can be quite tedious and expensive.

3. Small organic molecules

This section of our review is dedicated to the detection of small organic molecules. In this section, we will present recent studies on the detection of carbohydrates, amino acids, organophosphorus compounds, fluorescence dyes, antibiotics, and small biomolecules. The detection of such small molecules is of the utmost importance in both medicine and biochemistry, with applications in drug discovery, disease detections, and clinical screenings. The list of respective studies with additional information can be seen in Table 1, in addition to works for metal ions.

3.1. Small biomolecules

The first detection of a small molecule using SEF was performed in 1997, by the research group of Dr. Fritz Pittner [16]. They utilized silanized silver island films to investigate the mechanism of SEF between metal and fluorophore and to gain insight into the process of fluorophore attachment. They used fluorescein isothiocyanate (FITC) as a fluorophore and found that fluorescence emission increases 14 times in the presence of silver island film, and after 100 nm the intensity of emission rapidly decreases, which was attributed to concentration quenching. These insights paved the way for further investigations and developments of more complex detection techniques based on SEF.

In the late 2000s and early 2010s, two research groups showcased the use of novel nanostructures for the detection of complex small organic molecules. The first is the group of Dr. Perish Chandra Ray, which, after a successful detection of metal ions in 2008, presented a new approach for the detection of organophosphorus agents using gold nanoparticle applied surface [39]. They achieved a 1 μM limit of

Table 1
List of studies for metals and small organic molecules.

Authors et al.	Analytes	Concentration range	LODs	Substrate and exc. λ	Other analytical parameters
Gopala Krishna Darbha [34]	Hg (II) ions	0,8–170 ppb	2 ppt	AuNP-based surface energy transfer probe, 532 nm	Rsq – 0.99, up to EF - 1100
Ning Sui [35]	Hg^{2+}, Ag^{+}, and coralyne	0–100 nM	Hg2+ 1,4 nM Ag+, and coralyne - 20 nM	Ag@SiO_2-DNA, 550 nm	EF - 2.5, Max Rel. Error 5.5% (av. 3.0%), Rsq – 0.9848 and 0.995
Zhenpeng Zhou [36]	Hg^{2+}	1–80 nM	1 nM	Thiol-DNA functionalized AgNPs, 495 nm	EF - 5, Recoveries. (101 ± 4) % and (93 ± 4) %
Baowen Sun [37]	Cu^{2+}	1–5 μM	0.3 μM	core–shell Ag-nanocube@SiO2@PMOs nanocomposite, 500 nm	EF – 3,
Linlin Liang [38]	Pb^{2+}	1 pM - 3 μM	0.3 pM	$ZnFe_2O_4$ @Au-Ag Comp. and DNA/CeO_2 complex, 360 nm	lg(I562/I424) = −0.2713lgc – 2.312 (R2 = 0.995), RSD – 3.8% and 4.6%
Thomas Schalkhammer [16]	Fluorescein isothiocyanate	NA	NA	Si-SiFs, 488 nm	EF – 14
Samuel S.R. Dasary [39]	Organophosphorus agents	1–25 μM	1 μM	AuNPs, 395 nm	Rsq 0.99, EF - 5
Fu Tang [19]	PFV	NA	NA	Ag@SiO_2 NPs, 405 nm	EF – 1.3
Ying Wang [40]	Adenosine	200 nM - 200 μM	48 nM	AgNP aptasensor, 532 nm	Rsq = 0.995, y = 0.395× + 0.3668
Yaodong Zhang [41]	Paraoxon and Tacrine	0.5 μM–10 μM Paraoxon, 15 nM to 120 nM Tacrine	0.4 μM – Paraoxon, 10 nM - Tacrine	AuNPs modified with DDAO-AChE, 447 nm	EF - 6, RSD 1.7% Paraoxon, 2.1% Tacrine
Yecang Tang [42]	Glucose	2–52 mM	1,86 mM	AgNP-CdSe QD, 400 nm	EF – 9, Rsq = 0.991, RSD – 1.4%
Eunji Gang [43]	Glucose	1 μM – 1 mM	50 nM	Ag@SiO2-entrapped hydrogel microarray, 580 nm	EF – 4, Rsq = 0.997, RSD – 6.5%
Tian Tian [24]	Ascorbic acid	0.2–60 μM	25 nM	Ag-CD nanohybrid, 500 nm	Rsq = 0.986, Recoveries 92–106%
Ramar Rajamanikandan [44]	Dopamine	20–220 nM	0,35 nM	GSH-Ag nanoclusters, 490 nm	EF – 100, S/N – 3, Recoveries 96–98%
Qiao Cheng [45]	Heparin	0.025 to 2.5 μM	8.2 nM	Ag-g-CNQDs, 450 nm	ΔF = 133.4C + 25.18 (Rsq = 0.99)
Krishanu Ray [47]	Sulforhodamine B (SRB)	NA	NA	SIFs, 514 nm	EF – 7
Kadir Aslan [46]	Rhodamine 800	NA	NA	Ag@SiO_2 NPs	EF – 20
Lu Lu [48]	ATP	0–0,5 mM	8 μM	Ag@SiO2 nanoflare	EF – 32, Recoveries 89–94%
Kaiyu Wang [49]	ATP and thrombin	ATP 10 nm - 100 μM Thrombin 0,1 nm - 100 nm	ATP - 1,3 nM Thrombin - 0,073 nM	SIFs, 473 nm	Rsq = 0.995 and 0.997 RSD – 3.8% and 5.2%
Quanwei Song [50]	ATP	100 nM – 5 mM	14.2 nM	Ag@SiO2NPs with PG/dsDNA complex, 482 nm	Rsq = 0.998, Y = 0.102× + 0.888
Mustafa H. Chowdhury [5]	Tryptophan and Tyrosine	NA	NA	AlNPs, 280 nm	EF > 3500
Henryk Szmacinski [52]	Tryptophan residues in proteins, avidin	120 to 180 ng/cm^2	submonolayer of avidin of less than 2 ng/cm^2 was detected	SIFs, 280 nm	EF – 2-3 and 6.4
Hongliang Tan [53]	Tetracycline	10 nM – 10 μM	4 nM	AgNPs with Eu^{3+}, 390 nm	EF – 4, Rsq – 0.991, RSD – 0.26-0.67%
Xiaoming Yang [54]	Tetracycline	0,01–5 μM	4 nM	DNA-templated Au nanoclusters, 375 nm	S/N – 3, Rsq = 0.99
Sheng-Nan Yin [55]	ciprofloxacin (CIP), enrofloxacin (ENR) and lomefloxacin (LMF	0.025 to 1.0 mg/L, 5.0 to 160 ng/L and 0.01 to 0.8 mg/L	90, 5 and 6 ng/L	AgNPs, 277–285 nm	RSD <1.2%, Rsq > 0.998
Long Yu [56]	Doxycycline	0,5–2,5 μM	47 nM	MOF, 365 nm	Rsq = 0.998, Recoveries. 105.5% and 109.5%, RSD – 1.1%-2.1%
Bing Tan [57]	Oxytetracycline	0,5–5 μg/L	0,4 μg/L	2D MOF-DNA nanosystem	The slope of linear range – 0.0399

Exc. λ -excitation wavelength; Rsq – correlation coefficient; EF- fluorescence enhancement factor; RSD – relative standard deviation; CD- carbon dot; QD – quantum dot; Comp – composite; SIFs – silver island films; MOF – metal-organic framework; NA – not available.

detection in the range between 1 and 25 μM. They used Eu^{3+} ions as the fluorescent agent, which are released from the surface of AuNPs in the presence of organophosphorus agents. Conversely, the group led by Dr. Li used poly[9,90-bis(600-(*N*,*N*,*N*-trimethylammonium)-hexyl) fluorene-2,7-ylenevinylene-*co*-*alt*-1,4-phenylene dibromide] (PFV) as a fluorophore [19]. They attached this conjugated polymer to silver core-shell nanoparticles and obtained an enhancement of fluorescence signal of 1.3, as compared to this polymer on the silica surface. The next year, the group led by Dr. Chen developed a new aptasensor with silver nanoparticles for the detection of adenosine [40]. They achieved a 48 nM limit of detection, with a concentration range from 200 nM to 200 μM, and a correlation coefficient of 0.9949. In addition, this aptasensor showed high selectivity towards adenosine in the presence of other nucleosides. In the following year, the group of Dr. Zhang performed a

series of experiments to test their newly designed AuNPs-based sensor for the detection of acetylcholinesterase (AChE) inhibitors [41]. This sensor is based on the combination of gold nanoparticles with a 7-hydroxy-9H-(1,3-dichloro-9,9-dimethylacridin-2-one) (DDAO) fluorophore bound to AChE. This structure gives the opportunity to selectively detect AChE inhibitors with high sensitivity. The results of the experiments showed a 0.4 μM limit of detection for paraoxon and a 10 nM LOD for tacrine, with 6-fold fluorescence enhancement. With such advancements in fluorophore and substrate modification, further research in this area has become more prominent.

Consequently, in the following years, with the development of quantum dots and more complex nanostructure substrates, the number of research publications for these types of molecules has increased. As an example, the group of Dr. Tang in 2014 showed the application of the AgNP-CdSe quantum dot complex for the detection of glucose [42]. They obtained a limit of detection of 1.86 mM by measuring the concentration range between 2 and 52 mM. Moreover, they found that the presence of silver nanoparticles increases the fluorescence emission of quantum dots 9 times and produces a clear hypsochromic shift. Next year, the group of Dr. Koh used the same analyte to test the applicability of their novel Ag@SiO2-entrapped hydrogel microarray [43]. The main idea behind their sensor was to trap the enzymes and core-shell NPs in the poly(ethylene glycol) hydrogel to overcome issues of leaching and activation. They were able to achieve 4-fold fluorescence enhancement and a 50 nM LOD with a concentration range from 1 μM to 1 mM. With the further development of carbon dots, the group of Dr. Song performed a study utilizing a silver – carbon dot nanohybrid for the detection of ascorbic acid [24]. They were able to obtain a 25 nM limit of detection using a concentration range between 0.2 and 60 μM. It should be noted that this nanohybrid was capable of application in near-infrared to blue emission. In the same year, the group of Ramar Rajamanikandan and Malaichamy Ilanchelian showed selective and sensitive detection of dopamine using glutathione coated silver nanoclusters [44]. The respective TEM image of the substrate used in their biosensor can be seen in Fig. 1.

Moreover, the spectra for the concentration range between 20 and 220 nM can be seen in Fig. 1, in addition to the respective calibration plot. The limit of detection of dopamine for this substrate was found to be 0.35 nM. Additionally, common interferents like uric acid, ascorbic acid, metal ions, and anions did not have a negative effect, even in 100-fold concentrations. The next year, the group led by Dr. Song conducted a study of silver nanoparticle composites with carbon nitride quantum dots for sensitive detection of heparin [45]. The main strategy of this study was to bind polyethylenimine (PEI) to a nanoparticle-quantum dot complex in order to decrease the fluorescence emission. Subsequently, the heparin molecule would be able to extract PEI molecules due to the higher affinity of PEI to heparin, thus increasing the fluorescence emission. These innovative substrate modifications paved the way for new applications of MEF in biosensing.

The highest EF among these research studies was achieved by the group of Dr. Ilanchelian by using glutathione protected silver nanoclusters for the detection of dopamine [44]. This assay also showed the lowest limit of detection, at 0.35 nM. The main advantage of this method is its high selectivity, as even 100-fold concentrations of bioactive molecules did not produce an interfering signal. This setup was also used for the quantification of a human urine sample and showed good results. These results come from an increase in fluorescence intensity due to hydrogen bonding between the sensor and dopamine. However, this interaction can be degraded in the presence of a hydrogen-bonding molecule with a higher affinity to glutathione, thus decreasing the efficiency of this method. Nevertheless, this setup has shown to be highly selective and sensitive to dopamine in experimental conditions and real-life samples.

3.2. Rhodamines and ATP

In 2007, the group of Lakowicz and Geddes performed a series of experiments on the detection of rhodamine fluorescent dyes using silver island films and core-shell silver nanoparticles as substrates [46,47]. In the case of SIFs substrate, they obtained a 7-fold increase in fluorescence emission and reduced fluorescence lifetimes. Building upon this investigation, they obtained a 20-fold increase in fluorescence intensity by utilizing silver core-shell nanoparticles and a decrease in the fluorescence lifetime. These research works showed the capabilities of these substrates for enhancement of fluorescence signal and the nuances that should be accounted for.

More recently, in 2014 and 2015, there were research works on the same SIF and silver core-shell nanoparticle substrates. However, the analyte of choice was adenosine triphosphate (ATP). This compound is an essential part of every living organism and crucial for research in metabolic activities and kinetics. In 2014, the group of Dr. Zhang performed the detection of ATP using core−shell Ag@SiO2 nanoflares [48]. In this work they showcased the procedure for the synthesis of core−-shell Ag@SiO2 nanoflares; the result of this procedure can be seen in Fig. 2, on the TEM images of respective nanoflares. They then performed a series of experiments on the detection of ATP. In Fig. 2B, we can observe two calibration plots for fluorescence intensity and fluorescence ratio. The range of concentration was from 0 to 0.5 mM and the limit of detection was 8 μM. Moreover, the selectivity experiment showed a high affinity of this probe for the analyte of interest.

In 2015, the group of Dr. Tan and Dr. Lan showed an even lower limit of detection by utilizing PicoGreen (PG) signal molecule and SIF

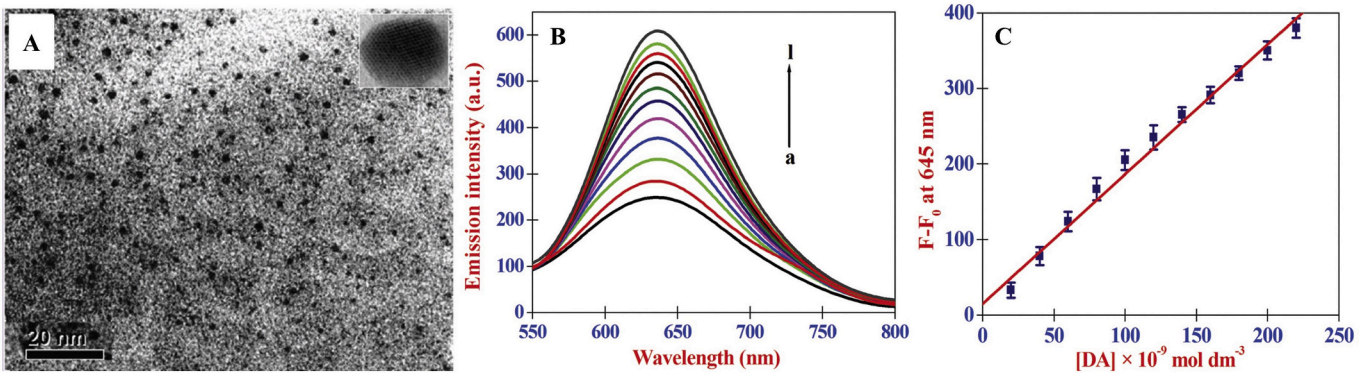

Fig. 1. (A) Representative HR-TEM image (inset: single GSH-AgNCs); (B) Emission spectra of GSH-AgNCs in the absence and presence of different concentrations of DA [DA]: (a) 0.00, (b) 20.00109, (c) 40.00109, (d) 60.00109, (e) 80.00109, (f) 100.00109, (g) 120.0109, (h) 140.00109, (i) 160.00109, (j) 180.00109, (k) 200.00109 and (l) 220.00109 mol dm3 and (C) corresponding calibration plot. (lemi = 645 nm, lexi = 490 nm) pH = 8.0 in PBS; Reprinted by permission of Royal Society of Chemistry, Rajamanikandan et al. [44].

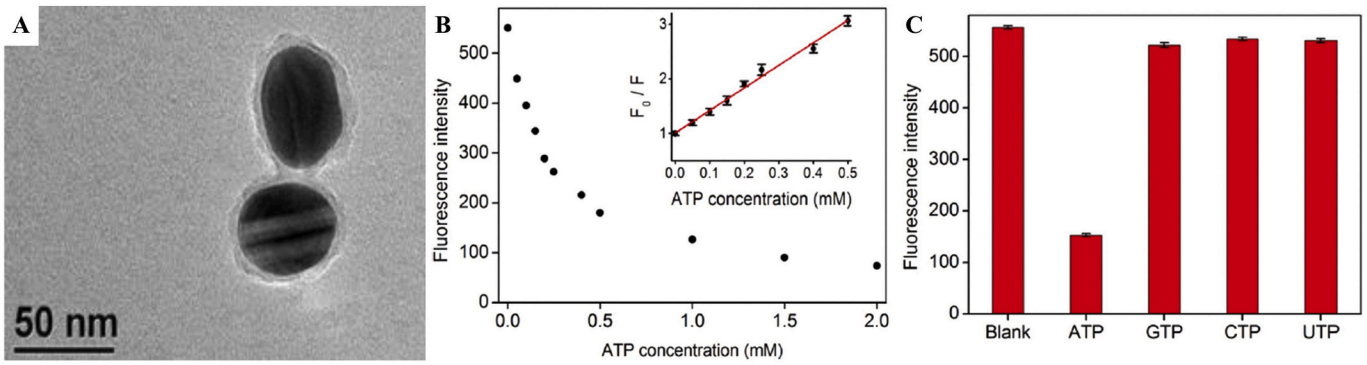

Fig. 2. (A) TEM images of the core−shell Ag@SiO2 NPs with 8 nm shell thickness; (B) Plot of the fluorescence intensity at 670 nm of the nanoflare versus the various ATP concentrations. The inset shows F0/F versus the ATP concentration from 0.0 to 0.5 mM. F0 and F are the fluorescence intensities in the absence and presence of ATP, respectively. (C) Selectivity test for ATP. The ATP concentration is 0.5 mM. Each data point represents the average value of three independent experiments with error bars indicated; Reprinted by the permission of American Chemical Society, Lu et al. [48].

substrate [49]. In a concentration range from 10 nM to 100 μM, they obtained an R-squared value of 0.995 and a limit of detection of 1.3 nM for ATP. Moreover, they performed a similar experiment for thrombin and achieved even better results, with a 0.073 nM detection limit. Additionally, they conducted reproducibility tests for the detection of ATP and obtained 3.8% intra-assay reproducibility and 5.2% inter-assay reproducibility. In the same year, the group of Dr. Ouyang conducted a similar experiment with the PicoGreen indicator but with silver core-shell nanoparticles [50]. This aptasensor was able to achieve a limit of detection of 14.2 nM, with a concentration range from 100 nM to 5 mM and a correlation coefficient of 0.998. Overall, these works showcased the successful detection of ATP with completely different approaches based on the same principles of MEF.

The highest EF in this chapter was shown by the group of Dr. Zhang with core−shell Ag@SiO2 nanoflares [48]. The lowest limit of detection was reported by Wang et al. [49]. Both studies try to quantitatively detect andn measure ATP; however, their approaches are quite different. Core−shell Ag@SiO2 nanoflares were used for the highest EF and a PG signal molecule-SIF aptamer complex was used for the lowest LOD. The difference in EF can be explained by higher fluorescence enhancement capabilities of silver core-shell nanoparticles as compared to silver island films. Nevertheless, both methods are highly sensitive, as they utilize ATP specific aptamers and can use other biomolecule specific aptamers. However, it can be noticed that the robustness of Ag@SiO2 nanoflares is higher compared to that of silver island films, as the silicon oxide layer shields the silver core from damage. Overall, both methods show the importance of aptamers for biosensing and how they can be incorporated into MEF biosensors.

3.3. Amino acids and antibiotics

With the development of better MEF substrates, the variety of molecules that can be analyzed and detected by this method has risen steadily. Two important molecules of interest were amino acids and antibiotics, as the former is an essential building block and signaling structure of every organism, and the latter is a crucial component of our everyday life. Examples for the detection of amino acids were performed by the group of Dr. Lakowicz in 2009. They first tried label-free detection of tryptophan and tyrosine by a substrate made up of aluminum nanoparticles [51,52]. They then conducted the same experiment with a slightly different approach, using SIFs as a substrate. In the first experiment, they achieved a maximum of 3500-fold enhancement of fluorescence signal, in comparison with a glass substrate and significant emission enhancement in the 100–450 nm wavelength range. In the second experiment, they obtained 2 ng/cm^2 detection of the protein layer containing tryptophan molecules in the UV-blue range. These results showed the possibility of using different nanostructures for the sensitive detection of amino acids and the ability of conducting label-free assays using these sensing platforms.

The detection of antibiotics is essential for pharmacokinetics and drug discovery. Research works conducted in 2012 and 2014 used conventional gold and silver nanostructures whereas more recent research works concentrated on metal-organic framework (MOF) substrates. In more detail, the group of Dr. Chen showcased lanthanide modified silver nanoparticles for the detection of tetracycline in milk [53]. They combined innate fluorescence of Eu^{3+} lanthanide and fluorescence enhancement of AgNPs. This combination was able to achieve an LOD of 4 nM, with a linear range from 10 nM to 10 μM and a correlation coefficient of 0.991. Moreover, 4-fold fluorescence enhancement, as well as high selectivity for tetracycline, was reported. Similarly, the group of Dr. Yang obtained a remarkable 4 nM detection limit for tetracycline antibiotics in the concentration range between 0.01 and 5 μM [54]. This method was presented as an inexpensive, simple, and sensitive way for the detection of tetracycline in urine and milk. In the following years, the group of Dr. Wang conducted a series of experiments for the detection of fluoroquinolones with silver nanoparticles [55]. They performed detection of three fluoroquinolones: ciprofloxacin (CIP), enrofloxacin (ENR), and lomefloxacin (LMF). They obtained a limit of detection lower than 90 ng/L, with a concentration range from 5 ng/L to 1 mg/L. The correlation coefficient was higher than 0.998 and the relative standard deviation was lower than 1.2%. In comparison with conventional methods, this MEF-based platform showed at minimum, a 2-fold enhancement of the LOD. In 2020, Dr. Wang's and Dr. Zhao's groups separately performed a series of experiments on antibiotics by using more innovative substrates [56,57]. The former group used MOF with pyromellitic acid and europium for the detection of doxycycline, while the latter group applied the MOF-DNA nanosystem for the detection of oxytetracycline. Dr. Wang's group achieved a 47 nM detection limit, with a concentration range of 0.5 to 2.5 μM and with an R-squared value of 0.998. Conversely, Dr. Zhao's group obtained a 0.4 μg/L detection limit for oxytetracycline using the 2D MOF-DNA nanosystem. This research group paid more attention to the strategies and physical properties needed to produce the DNA nanosystem, which can be used even with nanostructures that have a low affinity for DNA. Dr. Zhao's group achieved a linear response in the analyte range of 0.5 to 5.0 μg/L, and obtained an aptasensor which possesses notable specificity and anti-interference ability.

In this chapter, the lowest limit of detection was shown by two separate research groups for the detection of tetracycline. The first group, led by Dr. Chen, utilized silver nanoparticles modified with Eu^{3+} ions [53]. They achieved a 4 nM LOD, with high selectivity against other bioactive molecules. The second group led by Dr. Yang also reported a 4 nM LOD by using a similar approach of combining Eu^{3+} ions with nanoparticles; in this case, they used gold nanoparticles. Because gold

has a higher robustness than silver, the authors were able to test the applicability of this sensor in human urine and milk samples. However, both methods have one main disadvantage, which is the high cost of lanthanide ions.

4. Proteins

Qunatitative SEF studies of proteins are summarized in the Table Two below.

In this section, we will direct our attention towards the molecules known as the building blocks of life – proteins. A list of studies that showcased the detection of these molecules can be seen in Table 2. Throughout the development of analytical chemistry, the detection and characterization of proteins was of utmost importance, since information about proteins can be used for drug discovery, disease detection and monitoring, research on metabolism, and all of biochemistry. We will start from proteins of a low molecular weight and build our way up to enzymes, hormones, and growth factors.

4.1. Proteins

The first advancements in the detection of proteins by surface-enhanced fluorescence were made by the group of Drs. Lakowicz and Geddes in the early 2000s. They started by developing a sensing platform based on the coating of silver colloidal particles with a layer of SiO_2 [14]. This coating was used to protect surface plasmon absorption and

Table 2
List of studies for proteins.

Authors et al.	Analytes	Concentration range	LODs	Substrate and exc. λ	Other analytical parameters
Kadir Aslan [14]	Cy3-labeled streptavidin	NA	NA	Ag@SiO_2	EF – 3-5
Evgenia G. Matveeva [18]	cardiac marker myoglobin (Myo)	NA	below 50 ng/mL	SIFs, 532 nm and 651 nm	EF – 10-15
Mustafa H. Chowdhury [58]	phycobiliproteins	NA	NA	SiFs, 473 nm, and 633 nm	EF - 9
Kadir Aslan [59]	Troponin I	1 ng/L – 100 μg/L	5 ng/L	silver nanoparticle films (SNFs), 473 nm	Time to detect 1 min
Cheng-Han Chao [60]	human cofilin-1 recombinant protein	1–10^5 pg/ml	1 pg/ml	streptavidin conjugated AuNPs, 632.8 nm	Rsq = 0,9845
Deep Punj [61]	cellular protein Annexin 5b, cell-wall surface protein A	NA	10 μM	Au plasmonic nanoantenna in a box, 633 nm	Detection volume 58 zl, EF up to 1100
Krishanu Ray [62]	streptavidin-conjugated Alexa-647	NA	NA	Au Klarite with AgNPs, 638 nm	EF - 50
Ping Ping Hu [63]	Prion protein	0.05–0.30 nM	NA	Ag@SiO2 with dual aptamer, 460 nm	EF – 3, F = 14.44 + 113.29 × cPrP(nM), Rsq = 0.992
Masahiro Tsuneyasu [64]	interleukin 6	2–50 pg/ml	2 pg/ml	Plasmonic chip, 632.8 nm	NA
Yuanfeng Pang [65]	rHA protein of the H5N1 influenza virus	dynamic range 2–200 ng/mL linear range 2–100 ng/mL	2.0 ng/ml	Ag@SiO_2 NPs, 482 nm	EF – 6.4, Recovery 105%, 30 min TTD
Zhu Chen [66]	lactoferrin	0.2 ng/ml to 25 μg/ml	0.1 ng/ml (1.25 pM)	Ag_{10}NPs with aptamers, 488 nm	Rsq = 0.998
Dangdang Xu [67]	alpha fetal protein (AFP)	0,5 pg/ml - 5 ng/ml	94.3 fg/mL	CDs, 360 nm	Rsq = 0.992 F = 50.5374 logC+197.8480, EF – 17.2
Naumih M. Noah, [68]	inducible nitric oxide synthase	86.4 pg/ml – 54 ng/ml	0.169 pg/ml	MED immunosensor	Recoveries 85% and 88.5%
Keiko Tawa [69]	soluble epidermal growth factor receptor	700 fM – 10 nM	700 fM	plasmonic chip, 632.8 nm	EF – 300, 10 min TTD
Hui Li [71]	platelet-derived growth factor-BB	16 pg/ml - 50 ng/ml	3.2 pg/ml	AgNPs and Ag@Au core–shell NPs, 532 nm	Recoveries 80.5%, 94.3%, 103.7%, EF – 10.8
Dong Zhu [70]	vascular endothelial growth factor-165	0.1 nM to 16 nM	0.08 nM	AgNPs with Mn-doped ZnS QDs, 585 nm	Rsq = 0.995, RSD – 3.3%, F = 0.1946 + 0.41670C
Ying Wang [72]	thrombin and platelet-derived growth factor-BB (PDGF-BB)	thrombin 55.6 pM - 13.5 nM PDGF-BB 625 pM - 20 nM	625 pM for PDGF-BB and 21 pM for thrombin	Aptamers modified AgNPs, 532 nm and 635 nm	Thrombin (Y1 = 336.86×-4.4419, Rsq = 0.997); PDGF-BB (Y3 = 57.765×-21.754, Rsq = 0.992)
Margarida M. L. M. Vareiro [73]	human chorionic gonadotrophin (hCG)	0 to 100 IU/ml	0.3 mIU/mL (6 pM)	SAM-streptavidin matrix, tethered to gold, 633 nm	Sensitivity 0.1 mIU/mL
Yi Wang [77]	f-PSA in HBS-EP buffer and human serum	0–10 pM	34 fM and 330 fM	Plasmonic chip, 632.8 nm	ΔF of 4% after 30 detection cycles and 4 days of operation, 30 min TTD
Robert Nooney [78]	polyclonal human IgG–goat antihuman IgG	0 to 10 ng/mL	0.086 ng/mL	AgNPs, 649 nm and 670 nm	EF 11–37
Hui Li [20]	IgE	0.49 to 7.8 ng/mL	40 pg/ml 211 fM	Aptamer/Oligomer/Cy3-AgNPs, 532 nm	Rsq = 0.983–0.997, RSD = 5.73%, EF – 36-126
Hui Li [79]	IgE	0.5–16 ng/ml	0.25 ng/ml	Cy5-AgNPs, 635 nm	EF > 25, Rsq = 0.979–0.997
Liangcheng Zhou, [80]	Protein A and human immunoglobulin G (IgG)	100 nM to 1 fM	300 aM	D2PA, with SAM of a molecular spacer, 785 nm	Av. EF – 7400, "hot spot" EF – 4 × 106
Xiaoming Yang [81]	carcinoembryonic antigen	0.01–0.1 ng/ml	3 pg/ml	AuNPs modified with thiolated DNA, 473 nm	S/N – 3, Rsq = 0.984, Recoveries 98.16%, 102.5%, 95.31%
Dang-Dang Xu [82]	prostate-specific antigen (PSA)	0.1–100 ng/ml	27 pg/ml	Ag@SiO2@SiO2-RuBpy, 450 nm	F = 16.10C + 139.31, Rsq = 0.998
Bartolomeo Della Ventura [83]	IgG in urine	10–100 μg/l	8 μg/L	AuNPs, 488 nm	LOQ – 11.5 μg/L

Exc. λ -excitation wavelength; Rsq – correlation coefficient; EF- fluorescence enhancement factor; RSD – relative standard deviation; CD - carbon dot; QD – quantum dot; Comp – composite; SIFs – silver island films; MOF – metal-organic framework; NA – not available; TTD – time to detect; MED – metal-enhanced electrochemical detection. SAM – self-assembled monolayer; LOQ – limit of quantification; S/N – signal-to-noise ratio.

decrease the probability of close-range metal quenching. The application of this new nanostructure was assessed by the detection of Cy3-labeled streptavidin and compared with non-coated identical silver colloids. Results showed that the SiO_2 coating increases fluorescence enhancement by 3–5 times and fluorescence from the biotin-streptavidin interaction was well observed. Building on this short investigation, the group proceeded with experiments on metal-enhanced fluorescence using SiFs in 2005 and 2007 [18,58]. In the 2005 experiment, the group tried the detection of the cardiac marker myoglobin using immunoassay procedure. They obtained a 10-15-fold enhancement of fluorescence signal for SiFs compared to the glass substrate and showed that it is possible to distinguish concentrations of myoglobin below 50 ng/ml, which is lower than clinical values. In the following years, they applied the same SiFs substrate for the detection of phycobiliproteins, for their possible use as a fluorophore. Results showed that the proteins deposited on the surface of SiFs produce 9 times larger of a fluorescence signal and a 7-fold decrease in fluorescence lifetime. With these two works, the capabilities of metal-enhanced fluorescence were widened and directions for further studies were set.

Examples of such studies started to appear in the early 2010s with the development of new plasmonic substrates and fluorescence techniques. The first such study was performed by the group of Dr. Aslan [59]. The group tried to use a combination of low-energy microwaves with silver nanofilms to detect troponin I, which can work as an indicator of myocardial infarction. They obtained a 5 ng/L limit of detection with a concentration range of 1 ng/L – 100 μg/L. The most outstanding parameter of the assay is the time needed for the whole assay detection process, as it took only 1 min to obtain these results. The next year, the group of Dr. Chou performed a series of experiments on biotin-streptavidin interactions with gold nanoparticles for the detection of human cofilin-1 recombinant protein [60]. The expression of this protein is directly connected with ischemic shock. The group tested the new gold substrate by performing immunoassays on 57 samples taken from ICU (Intensive Care Unit) patients and 8 taken from healthy patients. They obtained a limit of detection of 1 pg/ml using a range between 1 and 10^5 pg/ml. This result, in addition to the great linearity (R^2 = 0.9845), shows good potential for the application of MEF with sandwich immunoassay for the detection of ischemic attack in ICU patients. Further studies on the detection of proteins using MEF were conducted by the groups of Dr. Wenger and Dr. Lakowicz in 2013 [61,62]. The group of Dr. Wenger used a novel plasmonic "antenna-in-box" sensor for the detection of cellular protein annexin 5b and cell-wall surface protein A. They were able to achieve up to 1100-fold fluorescence enhancement compared to the glass substrate, with a 58 zeptoliter sample volume and 10 μM concentration. On the other hand, the group of Dr. Lakowicz modified a commercially available gold klarite substrate for surface-enhanced Raman spectroscopy (SERS) by coating it with silver nanoparticles and assessing it using streptavidin-conjugated Alexa-647 protein-dye. This experiment resulted in a 50-fold fluorescence enhancement compared to the glass substrate and better photostability of the analyte dye, with 5-fold shorter lifetimes on the plasmonic substrate. Concurrently, the group of Dr. Huang performed a series of experiments to test the applicability of their newly designed solution-based MEF sensing platform for the detection of prion proteins [63]. They developed novel MEF substrate dual aptamers with both detection and imaging properties. This platform produced a linear fluorescence response for prion concentrations from 0.05 to 0.30 nM and a correlation coefficient of 0.992. In addition, they reported 3-fold fluorescence enhancement and excellent selectivity towards the prion protein compared to a number of common proteins, glucosides, and amino acids. These findings perfectly showcase the applicability of MEF techniques in biodetection.

Recent papers performing detection of proteins report on the use of more advanced nanostructures compared to previous works. One such recent work showcases the research conducted by the group of Dr. Tawa, in which selective detection of interleukin-6 was performed using a novel plasmonic chip [64]. Interleukin-6 is a protein that acts as an indicator of lifestyle diseases, with a 2.41 pg/ml concentration in healthy individuals. The results of this work showed that this novel biochip can detect even lower concentrations than the healthy cut-off, with a 2 pg/ml limit of detection in the range between 2 and 50 pg/ml. Conversely, the group of Dr. Wang used more common silver core-shell nanoparticles covered with a SiO_2 layer [65]. This substrate was used for the detection of recombinant hemagglutinin rHA protein, which is an indicator of the H5N1 influenza virus. They achieved the selective detection of rHA protein both in buffer solution and in human serum, with detection limits of 2 and 3.5 ng/ml, a dynamic range between 2 and 200 ng/ml, and a linear range between 2 and 100 ng/ml. With these results, they showed the potential of simple silver core-shell nanoparticle aptamers for the sensitive detection of protein tags in real-life samples and point-of-care diagnostics of the H5N1 influenza virus. In the following years, the use of aptasensors and novel quantum dots became more popular. For example, the group led by Dr. Xu performed a highly sensitive detection of lactoferrin in milk powder by using silver enhanced fluorescence polarization [66]. They developed a novel aptasensor that combines silver decahedral nanoparticles with fluorescein isothiocyanate dye and split aptamers. This sensor achieved a 0.1 ng/ml (1.25 pM) limit of detection, with a concentration range from 0.2 ng/ml to 25 μg/ml, and a correlation coefficient of 0.998. Similarly, the group of Dr. Tang performed the detection of the protein using novel carbon nanodots as an SEF substrate [67]. The protein of interest, in this case, was an alpha fetal protein (AFP), which is an indicator of liver cancer, pancreatic cancer, lung cancer, and liver cirrhosis. The group was able to achieve a great linear response in the range of 5 orders of magnitude, from 0.5 pg/ml to 5 ng/ml, and a limit of detection of 94.3 fg/ml. The calibration plot of this analysis can be seen in Fig. 3, in which it is also possible to observe the SEM image of the substrate surface and the TEM image of the CDs deposited on the gold film surface. Furthermore, the selectivity study showed remarkable sensitivity only for the AFP protein, which can be seen in the selectivity plot from Fig. 3. Overall, the development of these novel substrates and techniques has led to notable increase in the variety of applications for protein detection where the MEF phenomenon is at the cornerstone.

In this chapter, the highest fluorescence enhancement of 1100 was shown by the group of Dr. Wenger [61]. They utilized a non-conventional gold plasmonic "antenna-in-box" substrate for the detection of cellular protein Annexin 5b and cell-wall surface protein A. Such high enhancement was possible due to the design of the substrate, which increases the magnitude of the MEF effect in the gap region. One of the main properties of this design is the extremely low analyte volume needed for sensitive detection. An analyte volume of 58 zl with a 10 μM concentration was enough to get a reasonable signal. The main disadvantage of this setup lies in the size of the gap (15 nm), as the analyte size should be less than 15 nm. Hence, the choice of the analyte is limited and the preparation of analyte with such a low volume can be problematic.

4.2. Enzymes, hormones, and growth factors

This sub-chapter will direct its attention to more specific proteins like enzymes, hormones, and growth factors. An example of enzyme detection was conducted by the group of Dr. Sadik, which used an ultrasensitive portable capillary (UPAC) fluorescence immunosensor for the selective and sensitive detection of inducible nitric oxide synthase [68].

With this sensor, they achieved a 1.05 pg/ml limit of detection, 3% selectivity, and 85% average recovery. The successful detection of this synthase leads to new methods of assessing NO levels for biomarker and clinical purposes. This example may not show a direct connection to the SEF phenomenon, but it illustrates the possibilities of similar plasmonic substrates and biosensors for the detection of more complicated proteins, and demonstrates new prospects for the application of SEF.

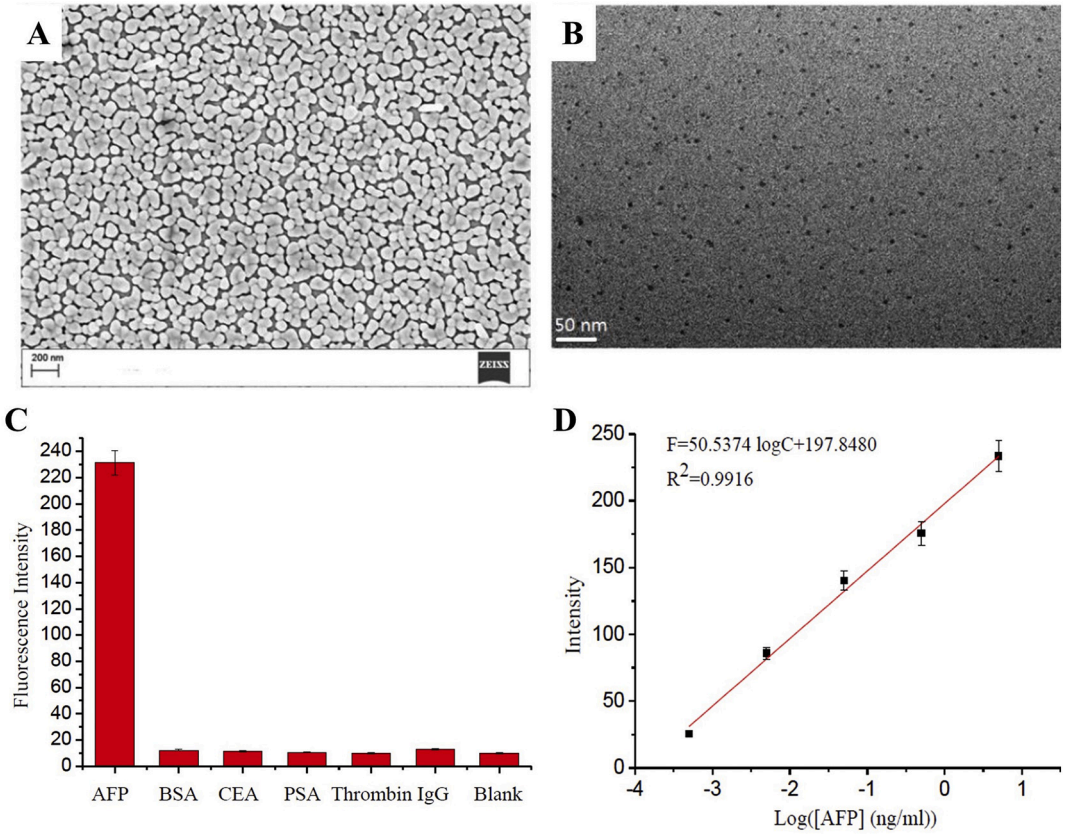

Fig. 3. (A) SEM micrograph of the plasmonic slide showing the nanoscale gold island morphology. (B) TEM micrograph of the CDs as-prepared. (C) Selectivity plot of the assay system. (D) Calibration curve for AFP detection (RSD < 5%); Reprinted by the permission of American Chemical Society, Xu et al. [67]. (For interpretation of the references to colour in this figure legend, the reader is referred to the web version of this article.)

The first example for the detection of growth factors is from the research group of Dr. Tawa, in which a new plasmonic biochip was constructed for the detection of soluble epidermal growth factor receptor [69]. This growth factor is one of the markers for tumor growth. The respective photo image of the plasmonic chip can be seen in Fig. 4, in addition to the scanning probe microscope image of the grating and cross-sectional scheme of the plasmonic chip. Using this novel substrate, the group obtained a 300-fold enhancement of fluorescence signal for this biochip as compared to the conventional ZnO-coated glass slide. Moreover, they achieved a detection limit of 700 fM within the range of 10 nM – 700 fM. Finally, this biochip showed great reproducibility and potential for an application in blood testing.

In the following years, the group of Dr. Zhang developed a time-resolved fluorescence sensor based on Mn-doped ZnS quantum dots with AgNPs [70]. This sensor was designed to detect vascular endothelial growth factor-165, which is a primary cancer biomarker. By using this sensor, the group achieved a 0.08 nM limit of detection in a concentration range from 0.1 nM to 16 nM, and a correlation coefficient of 0.995. Moreover, the modification of the sensor with AgNPs increased the sensitivity 11-fold due to the MEF mechanism.

Further examples concentrate their attention on the platelet-derived growth factor-BB (PDGF-BB), which is an indicator of tumor

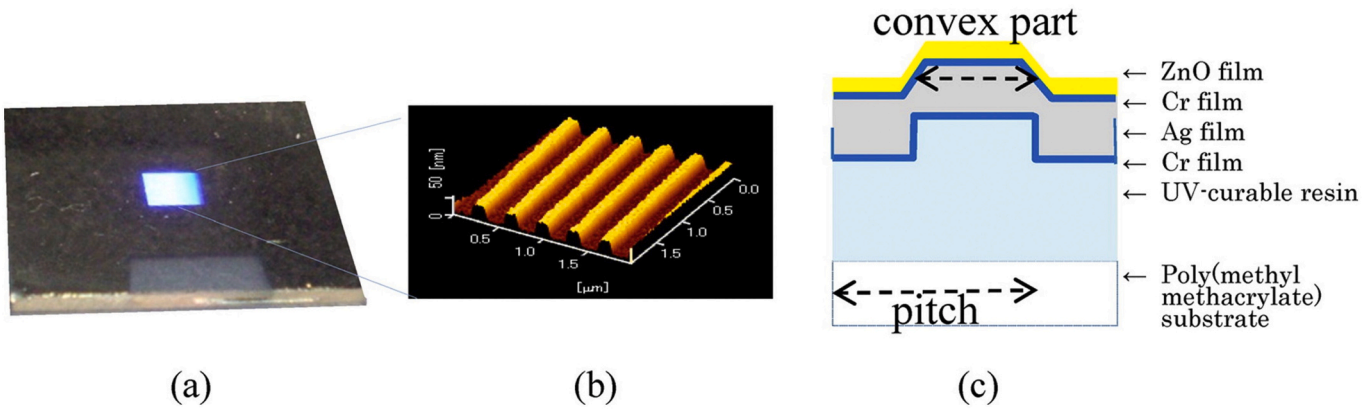

Fig. 4. Plasmonic chip: (a) photo image of the plasmonic chip, with the blue area corresponding to the grating; (b) scanning probe microscopic image of the grating coated with silver and ZnO films; (c) scheme of the cross-section of the plasmonic chip; Reprinted by the permission of American Chemical Society, Tawa et al. [69]. (For interpretation of the references to colour in this figure legend, the reader is referred to the web version of this article.)

angiogenesis. Both of these research works were conducted by the group of Dr. Xu and utilized modified silver nanoparticles [71,72]. In the first case, they used the AgNPs for the detection of PDGF-BB and the synthesis of Ag@Au core-shell nanoparticle arrays. The constructed substrate showed a significant increase in signal enhancement and a decrease in fluorescence lifetime. Moreover, the group achieved a 3.2 pg/ml detection limit with a linear range from 16 pg/ml to 50 ng/ml, and with an average recovery of approximately 90%. Building upon these findings, they performed the synthesis of new silver nanoparticles modified with aptamers for the detection of PDGF-BB. They were able to obtain a limit of detection of 625 pM for PDGF-BB, with a linear range from 625 pM to 20 nM. They also performed the detection of PDGF-BB without silver nanoparticles, and found that the addition of AgNPs significantly enhances fluorescence intensity, which directly correlates with an 8-fold decrease in the limit of detection. Overall, these novel applications of silver nanoparticles and MEF open new incentives for further developments of new aptamers and biosensor platforms, which consequently diversify the pool of analytes for this technique.

A different approach from other studies was taken by the group of Dr. Jenkins, which utilized surface-plasmon resonance and surface-enhanced fluorescence for the detection of the human chorionic gonadotrophin (hCG) hormone using gold nanoparticles modified by a layer of streptavidin [73]. They achieved the sensitive detection of 0.3 mIU/ml concentration of hCG in the range between 0 and 10 IU/ml, with 0.1 mIU/ml sensitivity. The importance of this work lies in optimizations of the biosensor with respect to antibody orientation and the position of the binding site.The highest EF of 300 and the lowest LOD of 700 fM were reported by the group of Dr. Tawa [69]. They achieved these results for the detection of soluble epidermal growth factor receptor by using a plasmonic chip. This plasmonic chip consists of the main plasmonic silver film coated with the ZnO layer, with Cr film in between. The high sensitivity of this method is due to the bispecific antibody modification of the plasmonic chip. The high enhancement factor can be attributed to the grating structure of the chip and the plasmonic properties of the silver film. However, to achieve such good properties and results, synthesis becomes quite difficult and expensive, as several sessions of sputtering and nanolithography are required. Nonetheless, such a novel design of the sensor can inspire more effective and less expensive biosensors.

4.3. Antibodies and antigens

The immunoassay is one of the most popular and irreplaceable analytical techniques in biosensing and medicine, as it provides reliable and sensitive detection of a variety of biological analytes through antibody-antigen relationships. The use of spectrophotometric techniques has significantly enhanced the sensitivity of immunoassays, especially fluorescence spectrophotometry [74,75]. Moreover, with the development of MEF, the number of different platforms combining immunoassays with fluorescence detection has increased. The list of such applications of MEF can be seen in Table 2. It can be observed from this table that one of the first examples in this area was performed in 1998 by the group of Dr. Cotton [76]. Dr. Cotton's group investigated the enhancement properties of newly developed silver colloidal films covered with silica layer through the detection of goat immunoglobulin and a conjugate of rabbit anti-goat immunoglobulin. They achieved a significant 20-fold enhancement of the fluorescence signal and demonstrated the first use of SEF for immunoassays. This research spurred several investigations and developments in the area of immunoassay biosensors in the following years. In 2009, two separate groups made valuable advancements in the field of surface-enhanced fluorescence immunoassays. The first research work was performed by the group of Dr. Knoll [77]. They conducted the synthesis and investigation of a novel biosensor for the detection of prostate-specific antigen (PSA). They achieved a 34 fM detection limit, with the concentration range of PSA spanning from 0 to 10 pM. Moreover, the average standard deviation of the sensor response was close to 4% after 4 days of operation and 30 cycles of detection. This example presented a highly sensitive and reproducible analytical platform for the detection of cancer antigen, and paved the way for future research in the design of biosensors. The second research work was conducted by the group of Dr. MacCraith [78]. They performed the detection of polyclonal human IgG and goat antihuman IgG using silver nanoparticles as a substrate. Using this nanoparticle, they achieved a 0.086 ng/ml detection limit, as well as a 0.95 positive correlation coefficient in the concentration range from 0 to 10 ng/ml. In addition, they found that the careful plasmonic tuning of nanoparticles and their uniform synthesis is crucial to the immunoassay's performance. These research articles show us that thorough preparation and characterization of substrates plays a major role in detection by SEF; this idea is manifested in more recent research works.

Examples of more recent works on the detection of antibodies and antigens can be taken from the beginning of the 2010s, with works from the groups of Dr. Chen, Dr. Xu, and Dr. Chou. The group of Dr. Chen conducted work on the application of the novel Cy3-modified silver nanoparticle aptamer/oligomer for the detection of IgE [20]. They obtained quite remarkable results: particularly, a 40 pg/ml or 211 fM limit of detection, with a correlation coefficient of 0.997 for an IgE concentration range of 0.48 to 7.8 ng/ml. These results demonstrated the possibility for the design of more complicated aptamers for the detection of biotags through surface-enhanced techniques. The group of Dr. Xu performed a similar experiment but with less complicated Cy3-modified silver nanoparticles [79]. This substrate achieved less radical results, with a 0.25 ng/ml limit of detection and a correlation coefficient of 0.996 for a 0.5 to 16 ng/ml range of IgE concentration. Nevertheless, one year later, the group of Dr. Chou performed the detection of human IgG using a three-dimensional nanoantenna-dot array modified with a self-assembled monolayer of molecular spacer [80]. The schematic representation of their novel substrate with and without an immunoassay, as well as SEM images of D2PA, can be seen in Fig. 5.

The research group achieved a 300 aM detection limit for a concentration range from 100 nM to 1 fM, where the dynamic range covers 8 orders of magnitude. It was calculated that a single-molecule of fluorophore placed in a "hotspot" of this substrate will produce a 4×10^6 – fold higher fluorescence signal. Combining all these works, we can clearly see a trend where advancement in substrate design increases the sensitivity and scope of correlated techniques and enables the detection of new analytes in different systems.

To continue with this topic, we will introduce three more research works that were done in the second half of the 2010s. The first work is performed by the group of Dr. Yang and concentrates on the detection of carcinoembryonic antigen with DNA modified gold nanoparticles [81]. The results of this study suggest that the modification of silver nanoparticles with gold nanoparticles with DNA enhances fluorescence enhancement and leads to an increase in sensitivity with a 3 pg/ml detection limit in the concentration range from 0.01 to 1 ng/ml.

Similarly, the group of Dr. Tang modified silver nanoparticles with a layer of silica oxide and fluorescent dye and assessed this nanoparticle by detection of PSA [82]. The results of this experiment can be observed in Fig. 6, where we can see the TEM images of the substrates; on the right, there is the fluorescence spectrum of PSA for the concentration range from 0 to 100 ng/ml, and a subsequent calibration plot. It is possible to see from the calibration curve that the coefficient of correlation is quite high and that there is a clear linearity present. The calculation of the limit of detection resulted in a concentration as low as 27 pg/ml to be detectable. This work sheds light on the possibilities for the construction of new dye embedded nanocomposites to be applied in bioassays.

The last example of this section is the work done by the group of Dr. Velotta in 2019 [83]. They synthesized an array of micropillars with clusters of gold nanoparticles attached to it. The assessment of this substrate was performed by the detection of human IgG in the urine sample. The results showed a good limit of detection for real samples (8

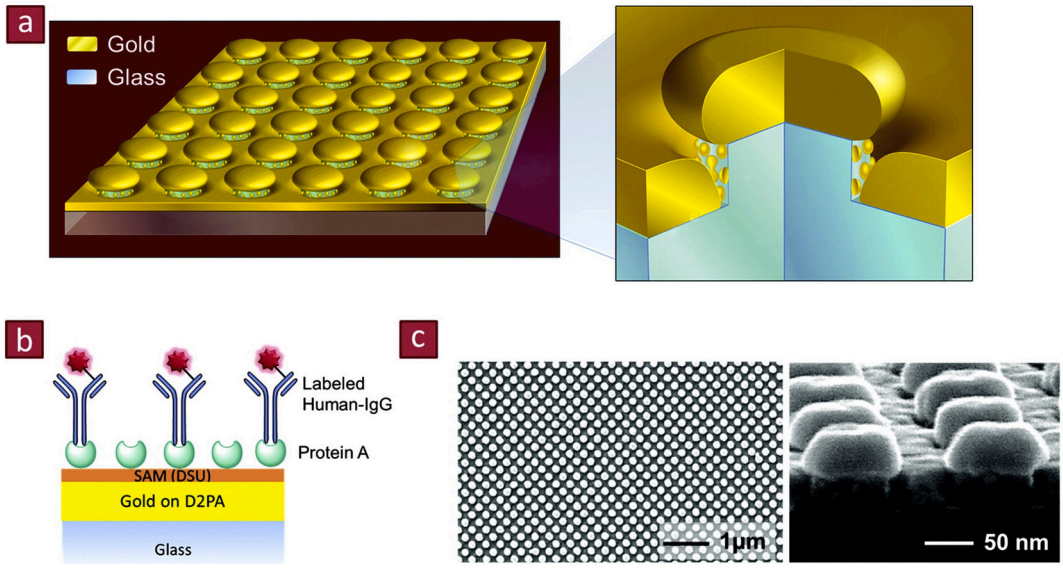

Fig. 5. (a) Overview and cross-section of the D2PA plate. (b) Schematic of the immunoassay on the D2PA (c) SEM images of D2PA with a 200 nm period (overview and cross-section); Reprinted by the permission of American Chemical Society, Zhou et al. [80].

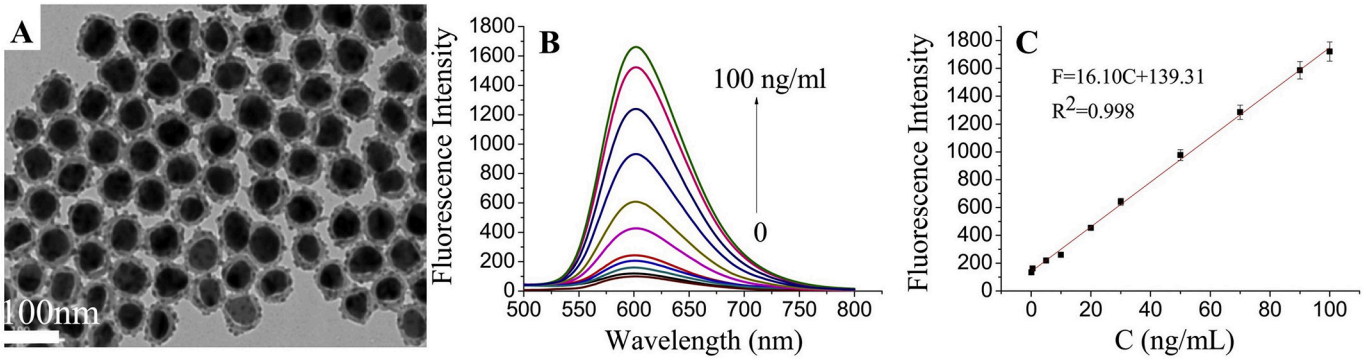

Fig. 6. (A) The TEM micrograph of composite nanoparticles Ag@SiO2@SiO2-RuBpy of 10 nm SiO2 spacer thickness; Fluorescence emission spectra of the detection system in the presence of an increasing amount of PSA and calibration curve for PSA detection. (B) Fluorescence emission spectra of the system upon the addition of different concentrations of PSA. (C) Calibration curve for PSA detection. Excitation: 450 nm; Reprinted by the permission of Elsevier, Xu et al. [82].

μg/L), with a linear range spanning from 10 to 100 μg/L. This sensor was suggested for point-of-care analysis of IgG in urine, backed by its sensitivity and reliability. Overall, all the methods and techniques discussed in this section showed remarkable results and provided insight into the development and design of novel substrates, to be used in fluorescent immunoassays.

The highest EF of 4×10^6 and the lowest LOD of 300 aM were reported by the group of Dr. Chou [80]. They achieved such remarkable results by using a highly ordered array of the golden disc-coupled dots-on-pillar antenna. This substrate was modified by the DSU SAM layer and protein A to detect and measure the concentration of IgG. The high enhancement and low LOD are caused by the 3D structure of the sensor, which increases the magnitude of the MEF effect and produces "hot spots". The modification by the SAM spacer layer also increases the effectiveness of this method. However, the fabrication of this sensor can be tedious and sensitive. Despite this, the D2PA plate synthesized by the group of Dr. Chou has excellent plasmonic properties and can be utilized in a variety of biosensing applications.

5. DNA, RNA, and oligonucleotides

Table 3 below summarizes SEF detection of DNA, RNA and oligonucleotides.

From the development of the first highly sensitive analytical techniques, the detection of DNA strands and oligonucleotides was of utmost importance. With the development of single-molecule-detection-capable spectroscopic techniques, the scope of such investigations has increased. Research in incorporating the SEF phenomenon for the detection of such molecules became quite popular, starting from the first examples at the beginning of the 21st century. Such examples and more are presented in this section and can be observed in Table 3 in greater detail. The first analytical detection of DNA/oligonucleotides was performed by the group of Dr. Knoll in the year 2000 [84]. They conducted a series of experiments on the detection of hybridization reactions of oligonucleotides using surface-attached probe DNA. They obtained a limit of detection of 1–5 oligonucleotide strands/mm^2, with a concentration range of analyte from 0.01 μM to 1 μM. This research helped to acquire insight into the surface hybridization mechanism of oligonucleotides and the kinetics of this process. Conversely, the work performed by the group of Dr. Gryzcynski is concentrated on the effect of metal nanoparticles on the intrinsic fluorescence of DNA, which is an essential first step to the application of SEF for the detection of DNA samples [17]. Dr. Gryzcynski's group used silver island films and achieved an 80-fold enhancement of the DNA fluorescence signal and a 3-fold decrease in fluorescence lifetime. These results sprouted numerous works in the area of DNA detection by SEF.

Table 3
List of studies for DNA, RNA, and oligonucleotides.

Authors et al.	Analytes	Concentration range	LODs	Substrate and exc. λ	Other analytical parameters
Thorsten Liebermann [84]	fluorophore-labeled 15mer target oligonucleotide	0,01–1 μM	1–5 oligonucleotide strands/mm^2	surface-attached probe DNA with SAM on Au, 632.8 nm	EF – 14.2
Joseph R. Lakowicz [17]	DNA	NA	NA	SIFs, 287 nm	EF – 15-2000
Kadir Aslan [85]	RNA	25–500 fmol	25 fmol	SIFs, 532 nm	$S/N > 20$ $n = 3$
Kadir Aslan [86]	DNA of *Bacillus anthracis* spores	40 to 4500 pg/μl	40 pg/μl	SIFs, 532 nm	S/N – 6, few minutes TTD
Larbi Touahir [87]	DNA hybridization	NA	5 fM	Ag, Au thin films, 550 nm, and 650 nm	EF – 10-20
Weibing Qiang [21]	DNA	12.8 pM - 40 nM	12,8 pM	AgNPs, 532 nm	EF – 2.4, ΔF = 6176log C - 5870 (Rsq = 0.9868)
Jia Chen [88]	hepatitis B virus DNA	1–800 nM	0,65 nM	SiO_2NP–DNA/Ag nanoclusters	RSD < 4,6%
Greggy M. Santos [89]	ERBB2 cancer gene DNA target	0–20 nM	1 nM	NPGD NPs, 532 nm and 785 nm	S/N - 123
Zhong Mei [23]	DNA	10 pM - 10 nM	10 pM	GNR biochip, 664 nm	Rsq = 0,99
Xiaofan Ji [90]	DNA	1 fM- 10 nM	0,01 pM	AgZNR arrays, 488 nm	EF - 28
Akash Kannegulla [91]	DNA	100 fM – 1 μM	300 fM	ORA with CdSe/ZnS QDs	EFs AgORA 42 and Ag substrate 11.8, sample volume 1.2 μL
Qingshan Wei [92]	DNA origami-based brightness standards	NA	~80 fluorophores per diffraction-limited spot	Ag-coated glass slide with a thin spacer, 465 nm	EF - 10
Linlin Liang [93]	miRNAs	0,1 to 6 fM	0.03 fM miRNA210 and 0.06 fM miRNA21	(FLS)-enhanced fluorescence/visual bimodal platform, 390 nm	ΔF = 126.80+ 96.48logCmiRNA210 Rsq = 0.9987, ΔF = 103.15+ 91.79logCmiRNA21 Rsq = 0.9966, RSD < 3%, Recoveries 96.88–103.0%
Jiajia Wang [94]	DNA marked with Rhodamine red	100 nM - 10 μM	10 pM	Au NPs/PSiMC device substrate, 530 nm	y = 1464,66 + 201,77C Rsq - 0,98 EF - 2

Exc. λ -excitation wavelength; Rsq – correlation coefficient; EF- fluorescence enhancement factor; RSD – relative standard deviation; CD- carbon dot; QD – quantum dot; Comp – composite; SIFs – silver island films; MOF – metal-organic framework; NA – not available; SAM – self-assembled monolayer; TTD – time to detect; LOQ – limit of quantification; S/N – signal-to-noise ratio; NPGD – nanoporous gold disk; ZNR – zigzag nanorod; GNR – gold nanorod; ORA – open-ring nanoarray; FLS – flower-like silver.

Building on the fundament laid by previously mentioned works, the group of Dr. Geddes performed a series of experiments on the detection of RNA and DNA. Both experiments were performed using silver island films, with the only difference being analyte nature. In the first work, they conducted an investigation on the capabilities of SiFs for the detection of DNA [85]. They obtained quite remarkable results, with a limit of detection of 25 fmol in the concentration range from 25 to 500 fmol. Moreover, they obtained a signal to noise ratio of 20, which indicates that the true limit of detection for this system is close to 5 fmol. After assessing the concept of MEF on RNA, they used this method for the detection of DNA from *Bacillus anthracis* spores [86]. They achieved a 40 pg/μl detection limit, with a signal-to-noise ratio of 6, in the concentration range of DNA from 40 to 4500 pg/μl. Henceforth, they showed the applicability of the newly developed substrates, and SEF as a whole, for the sensitive and selective detection of DNA and RNA.

This trend of new investigations and developments continued in the next decade, with works of groups led by Dr. Szunents and Dr. Xu in the early 2010s. The group of Dr. Szunents investigated the use of silver and gold films for the real-time detection of DNA hybridization using localized surface plasmon-enhanced fluorescence spectroscopy [87]. They achieved a limit of detection of 5 fM. They found that this substrate design can be used for highly sensitive detection of DNA and is capable of a thorough analysis of the hybridization process (including in-situ and real-time kinetics). This experiment led to a deeper understanding of the process and once again, demonstrated the applicability of surface-enhanced techniques for the detection of trace amounts of DNA. A similar experiment was performed by the group of Dr. Xu in 2013 [21]. The group conducted an experiment involving silver nanoparticles as substrates. The results showed that this substrate provides a signal enhancement of 2.4 and shows good linearity, with a correlation coefficient of 0.9868. The group's calculated limit of detection was equal to 12.8 pM. These promising results led to the development of more advanced MEF substrates and effectuated an increase in the variety and sensitivity of DNA detection.

As the technology of fabrication and the synthesis of more complicated and sophisticated substrates was being invented, the second half of the 2010s was met with a rapid increase in research articles. The first example utilizing novel substrates was presented by the group of Dr. Qiu in 2015 [88]. The group synthesized SiO_2NP-DNA/Ag nanoclusters for the detection of hepatitis B virus DNA. They obtained a 0.65 nM detection limit and a relative standard deviation of less than 4.6% for a concentration range of analyte from 1 to 800 nM. This proof-of-concept showed that such a substrate design can help negate background interference in complicated solutions and can detect a low concentration of hepatitis B virus DNA, both in aqueous buffer and in human serum. The next example concentrates on the detection of the ERBB2 cancer gene DNA target using nanoporous gold disk (NPGD) plasmonic nanoparticles [89]. Using this substrate model, the group was able to achieve a theoretical zeptomole detection limit, as the signal-to-noise ratio was 123 for a limit of detection of 1 nM in the concentration range from 0 to 20 nM. This experiment showed that the careful tuning of plasmonic properties and morphology of the substrate can lead to a potential single-molecule detection. Similarly, the group of Dr. Tang synthesized a highly ordered array of gold nanorods for the detection of trace DNA concentrations [23]. The experiment was conducted with a DNA concentration range from 10 pM to 10 nM. The resulting calibration plot showed a linear logarithmic relationship in this range, with a correlation coefficient of 0.9902. The limit of detection was calculated to be 10 pM. Most importantly, the group found that the distance between the fluorophore and the surface of the substrate greatly impacts fluorescence

enhancement, due to quenching and enhancement by metal nanoparticles. A similar substrate was introduced by the group of Dr. Fu – silver zigzag nanorod arrays [90]. Dr. Fu's group assessed this substrate by detection of the hybridization of trace DNA amounts. They achieved a 28-fold enhancement of fluorescence signal and a limit of detection of 0.01 pM. They also found that the folding number of zigzag nanorod arrays affects signal enhancement through a positive correlation, while the temperature of the substrate does not have any effect.

As recently as 2017, three groups led by Dr. Cheng, Dr. Ozcan, and Dr. Yan, respectively, researched the use of novel substrates for the detection of DNAs and RNAs. In particular, the group of Dr. Cheng performed the detection of DNA using open ring silver nanoarrays with quantum dots (QDs) [91]. The limit of detection for this system was estimated to be 300 fM, and 360 zmol if the volume of the sample is 1.2 μl. The group also obtained a 42-fold signal enhancement after the addition of quantum dots. This suggests that the addition of quantum dots can be applied to other systems to increase fluorescence enhancement. On the contrary, the group led by Dr. Ozcan designed a system based on a silver-coated glass slide, using a smartphone camera for the visual detection of DNA [92]. They achieved a detection limit of 80 fluorophores per diffraction-limited spot, and almost 10-fold enhancement of signal. This research showed the capabilities of metal-enhanced fluorescence for use in real-life applications in field-portable devices. Conversely, the group of Dr. Yan performed more lab-sophisticated detection of micro RNAs using a novel flower-like silver (FLS)-enhanced fluorescence/visual bimodal platform [93]. They achieved an extremely low limit of detection of 0.03 fM for miRNA210 and 0.06 fM for miRNA21, in the concentration range from 0.1 to 6 fM. In both cases, the calibration plots showed high linearity, with correlation coefficients of 0.9987 and 0.9966, respectively. They concluded with a proposition for the use of their modified substrate for other biomarkers and proteins. Last but not least, the group led by Dr. Jia published a research paper in 2018 on the detection of DNA marked with rhodamine dye using a porous silicon microcavity substrate embedded with gold nanoparticles [94]. The limit of detection was estimated to be 10 pM, with a concentration range spanning from 100 nM to 10 μM, and a positive correlation coefficient of 0.98. The authors noted that the performance of this substrate model is significantly better than the commercially available analytical tools used for the same purpose. This also suggests that with the development of newer and better substrates and preparation methods, we can observe an increase in real-life applications of SEF and the incorporation of this method into established analytical techniques. Overall, this positive shift is appearing not only for the detection of DNA and oligonucleotides, but for the entire spectra of biomarkers and organic molecules of interest.

The lowest LOD of 0.03 fM was reported by the group of Dr. Yan in 2017 [93]. The analyte of choice in this experiment was microRNA and the sensor was a flower-like silver enhanced fluorescence platform. The main advantage of this method, besides the low LOD, is its ability for multi-analyte detection. The use of flower-like silver increased the magnitude of fluorescence enhancement by MEF and FRET mechanisms, and decreased the platform's background fluorescence. In addition, this platform can be readily recycled in three cycles. However, the fabrication of the paper analytical device and its modification with flower-like silver is quite difficult and expensive.

6. Bacteria, viruses, and toxins

Table 4 below summarizes SEF detection of bacteria, viruses, and toxins.

This section is dedicated to analytes of a more complicated nature and a higher hazard level, like bacteria, viruses, and toxins. The detection of these analytes is of the utmost importance, due to the ongoing war with terrorism and the prevalence of infectious diseases caused by toxins, bacteria (tuberculosis, etc.), and viruses (particularly in the wake of the COVID-19 pandemic, which might become the most economically and socially devastating, if not the deadliest, pandemic in the last 100 years. All of these factors motivate the development of new diagnostic techniques, one of the most prominent ones being surface-enhanced fluorescence. With the development of more sophisticated substrates, applications of SEF in this area have rapidly increased in number. In this section, we will present several such applications discovered by various research groups around the world. A list of these applications can be found in Table 4 along with additional information.

It should be logical to start with less complex but important analytes - toxins. The first example of such an analysis was presented by the group of Dr. Geddes in 2012 [95]. They performed the detection of anthrax protective antigen (PA) exotoxin for its use in the presymptomatic diagnosis of *Bacillus anthracis*. As a substrate, they used a modified microwave-accelerated metal-enhanced fluorescence platform which consists of SiFs grown in a 96-well plate. With this setup, they achieved a limit of detection of 0.1 pg/ml and a lower limit of quantification of 1 pg/ml, for a range of concentrations from 0.01 pg/ml to 10 ng/ml. This approach not only appeared to be more sensitive than conventional ones, but the whole analysis took <1 h, which is significantly less than for other methods, and can be crucial in the case of lethal infection. The

Table 4
List of studies for bacteria, viruses, and toxins.

Authors et al.	Analytes	Concentration range	LODs	Substrate and exc. λ	Other analytical parameters
Anatoliy I. Dragan [95]	anthrax toxin (protective antigen)	0,01 pg/ml - 10 ng/ml	0,1 pg/ml	SIFs, 473 nm	LLoQ - 1 pg/ml, 40 min TTD, EF 200–400
Yun Li [96]	microcystin-LR	0.02–16 ng/mL	7 pg/ml	Au nano-crosses, 646 nm	Rsq = 0.9981, EF 2.3–35
Francesco Todescato [97]	Ochratoxin A (OTA)	NA	LOQ 3.6 pg/g	Ag–FON, 647 nm	EFs of $0.9 \pm 1 \times 10^4$ $14 \pm 6 \times 10^4$,
I. Abdulhalim [98]	*E. coli* (TV1061)	3.6×10^8 cfu/ml	NA	STFs made of Ag, Al, Au, Cu, 546 nm	EFs > 15
Chun-Jen Huang [99]	*E. coli* O157:H7	10–10^6 cfu/ml	10 cfu/ml	Plasmonic chip, 633 nm	40 min TTD, Rsq = 0.993
Syed Rahin Ahmed [22]	Influenza A virus targeting hemagglutinin (HA)	50–10,000 PFU/mL	50 PFU/mL	QDs and NPGL, 380 nm	EF – 2-9
Rostislav Bukasov [100]	*E. coli* (DH5α)	NA	NA	CDs made from date pits on Au film, 633 nm and 532 nm	S/N – 200, contrast – 66, EF - 50
Alisher Sultangaziyev [101]	*E. coli* (DH5α)	NA	NA	CdSeS/ZnS and CdTe alloyed QDs, 633 nm and 532 nm	EF – 450-480, contrast 360
Rostislav Bukasov [107]	*E. coli* (DH5α)	NA	NA	CDs made from date pits on Al foil and Al film	EF -35 contrast up to 200

Exc. λ -excitation wavelength; Rsq – correlation coefficient; EF- fluorescence enhancement factor; RSD – relative standard deviation; CD- carbon dot; QD – quantum dot; Comp – composite; SIFs – silver island films; MOF – metal-organic framework; NA – not available; SAM – self-assembled monolayer; TTD – time to detect; LOQ – limit of quantification; S/N – signal-to-noise ratio; STF – sculptured thin film: NPGL – nanoporous gold leaf; LLoQ – the lower limit of quantification.

next work is concerned with the sensitive detection of microcystin hepatotoxins. These toxins, produced by cyanobacteria, can contaminate water and other aquatic products. Exposure to these hepatotoxins is very dangerous, as it causes the fast deterioration of hepatic cells and consequently leads to death. The group of Dr. Qian attempted the detection of this toxin using novel Au nano-crosses with a cy5 fluorescence label [96]. They estimated that the limit of detection for this method is 7 pg/ml within the range of concentrations from 0.02 ng/ml to 16 ng/ml. Moreover, they found that the addition of gold nano-crosses increases signal intensity by 30 times, so the use of this sensing platform for the detection of microcystins in water and seafood was successful. A similar work was performed by the group of Dr. Bozio on the detection of Ochratoxin A (OTA), which is one of the most common food contaminants from the mycotoxin family [97]. This toxin is nephrotoxic, hepatotoxic, teratogenic, and immunotoxic. Dr. Bozio's group attempted the detection of this highly dangerous toxin using silver film over nanosphere (Ag-FON) plasmonic substrate, which has good signal enhancement and high robustness. With this setup, they achieved a limit of quantification of 3.6 ng/kg and 10^5 signal enhancement within the range of concentrations of OTA from 0.05 to 500 μg/kg. Overall, they demonstrated the potential of this sensor and of MEF technique for the sensitive detection of OTA. This technique is comparable to that of ELISA methods, but with improvements in the complexity of methodology and with a decrease in the analysis time.

Finally, we have covered chemical compounds and can now divert our attention to the most complicated analytes in this review of bacteria and viruses. The first example of bacteria detection was presented by the group of Dr. Lakhtakia in 2009 [98]. They used *E. coli* (TV1061) with a concentration of 3.6×10^8 CFU/ml, with metallic sculptured thin films (STFs) made of silver, aluminum, gold, and copper as substrates. They obtained a minimum of 20-fold fluorescence signal enhancement using this setup. Moreover, they found the crucial dependence of signal enhancement on the film's deposition angle, with lower deposition angles performing better. In the end, they concluded that this type of biosensor can be used for the detection of a variety of analytes in water samples. Similarly, the group of Dr. Knoll performed the detection of *E. coli* O157:H7 [99]. They used a gold surface modified with mixed thiol self-assembly monolayer (SAM) of PEG-thiol and COOH-thiol as a substrate and they utilized long-range surface-plasmon enhanced fluorescence spectroscopy. They achieved a detection limit below 10 CFU/ml, with a time to detect of 40 min., and with a concentration range of the analyte from 10 to 10^6 CFU/ml. Overall, they showcased the capabilities of this new biosensor with 3–4 orders of magnitude lower limit of detection compared to other used methods, and high specificity for the detection of specific strains of *E. coli* bacteria. On another note, the next example concentrates on the detection of the influenza virus. Virus epidemics are among the greates threats and chellenges to health systems across the globe, as we can see and feel today on a wake of COVID-19 pandemic. The group of Dr. Park and Dr. Lee performed the detection of influenza virus A/Beijing/262/95(H1N1) using quantum dots combined with nanoporous gold substrate [22]. The SEM and AFM images of this substrate can be seen in Fig. 7. They achieved a limit of detection of 50 PFU/ml, with a concentration range of the virus from 50 to 10,000 PFU/ml. Moreover, they found the logarithmic relationship between virus concentration and fluorescence intensity in the range of 1 ng/ml to 10 μg/ml, with corresponding calibration plots shown in Fig. 7.

In this experiment, the authors were able to showcase the ability of quantum dots for the detection of the influenza virus, with a considerable increase in signal enhancement when rougher plasmonic metal surfaces were used.

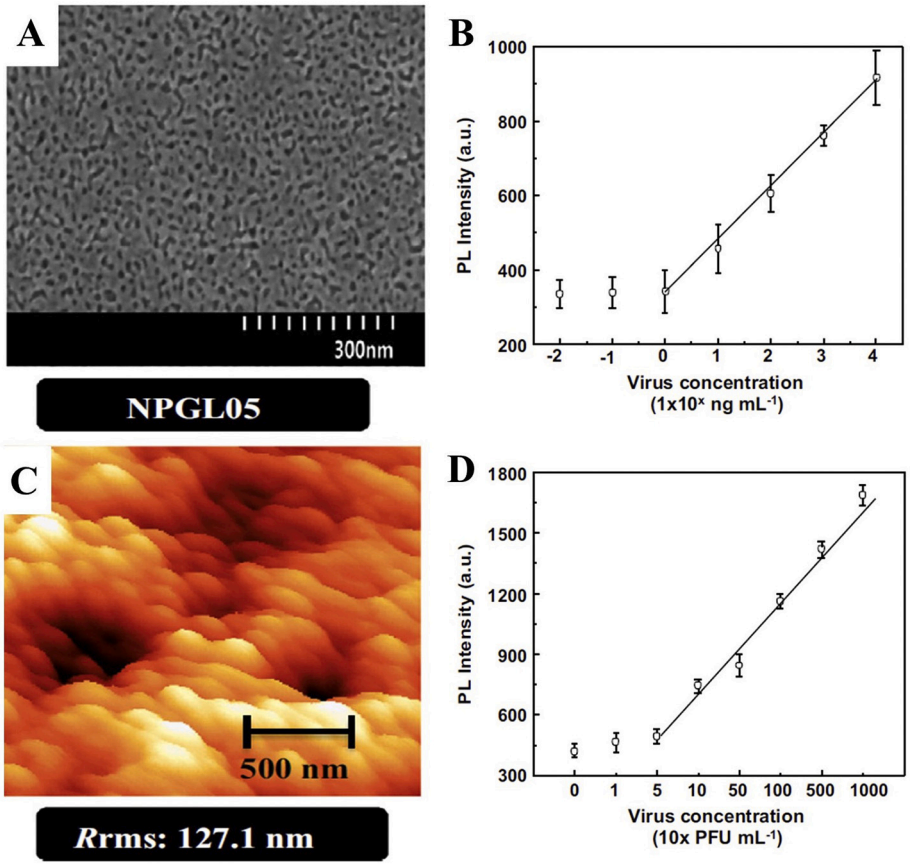

Fig. 7. (A, C) SEM and AFM images and the measured Rrms of NPGL sample; PL intensity versus influenza virus A/Beijing/262/95(H1N1) concentration; (B, D) The calibration curve of PL intensity corresponding to the concentration of the influenza virus A/Yokohama/110/2009(H3N2).The error bars in(B–D) indicate SD($n = 3$); Reprinted by the permission of Elsevier, Ahmed et al. [22]

Bukasov's group labeled *Escherichia coli* (DH5α) bacteria with carbon dots and quantum dots and observed SEF from single cells and cell agglomerates. Initially, carbon dots made from date pits were deposited on the surface of the gold film and compared to glass as the SERS substrates [100]. In this experiment, the signal-to-noise ratio was up to 200 and signal contrast (ratio of the signal of labeled cells to the signal of unlabeled (control) cells) reached up to 60; fluorescence signal enhancement relative to glass was about 50. Moreover, it was found that the excitation wavelength has a considerable effect on the fluorescence signal, with 633 nm excitation wavelength producing higher contrast than 532 nm laser. Next, we performed another experiment on the detection of *E. coli* (DH5α) bacteria, in which we used CdSe/ZnS alloyed quantum dots and CdTe core-type QDs on Al foil, Au film, Al film, silver and glass substrates [101]. Here, a significant increase in both signal enhancement and contrast was achieved, with values up to 450–480 and 360, respectively. In addition, the signal from the Al foil and Al film was about two times more reproducible than the signal from Au film. Finally, it was found that there was a strong negative correlation between QD and/or substrate toxicity for bacterial cells and fluorescent enhancement. Overall, we showcased the potential use of carbon dots and quantum dots for the sensitive detection of bacteria and introduced the use of Al foil as a potent substrate for the SEF detection of not only bacteria, but of any biological analyte.

The highest EF in this chapter was reported by the group of Dr. Todescato [97]. They achieved such high fluorescence enhancement by using silver film over nanosphere (Ag-FON) plasmonic substrate for the detection of Ochratoxin A. This high EF can be attributed to the structure of the substrate, which maximizes the MEF effect by aligning silver nanostructures in close proximity. This setup was also assessed by the detection of OTA in different food matrices. They obtained reasonable results that were lower than the specified concentrations of OTA according to the European Union. The main disadvantage of this setup was the non-linear response to a normal concentration range of OTA. In addition, increasing the labeling efficiency of the assay and the uniformity of the substrate surface remains a challenge.

7. Discussion of trends

Finally, we would like to discuss several trends that have surfaced during this mini-review. The first trend that we can observe is the increasing complexity of substrates and procedures over time for all analyte types. In the early years of protein detection, most research works concentrated on the use of silver-based substrates like silver island films [18,58] and silica-coated silver nanoparticles [14]. Later on, the use of more complicated gold and silver nanostructures, plasmonic chips, and carbon dots became more prominent [62,64,67,71,72]. A similar trend can be observed with articles on the detection of DNA, RNA, and oligonucleotides: in the 2000s, most attention was concentrated on plasmonic metal films, like silver island films [17,85,86]; it should be noted that most of the research in this area in the early 2000s was done by the group of Dr. Geddes. In the next decade, research began implementing more complicated substrates: nanoporous gold disks, gold nanorods, silver zigzag nanorods, flower-like silver platforms, and silver open ring arrays became more prevalent [23,89–91,93].

The next trend arises from analyte nature, and demonstrates that the increase in complexity of analytes requires more complicated substrates and procedures. This can be traced from the simple metal films and nanoparticles used for small organic molecules and proteins [18,22,34,39,58,60] to the complicated plasmonic chips, platforms, nanostructures, and quantum dots used for DNA sensing and detection of antibodies, toxins, and bacteria [77,82,94,97,99,101]. Furthermore, the last trend, arising from the differences between substrates and their increasing level of sophistication, states the following: the increase in the complexity of the substrate leads to better sensitivity and consequently, a lower limit of detection. For example, in the case of metals, we can observe that the LOD for Hg^{2+} decreases from 1.4 nM to 1 nM when more complicated Thiol-DNA functionalized AgNPs are used instead of $Ag@SiO_2$ NPs [35,36]. Moreover, this trend can be seen with proteins, where more old-fashioned silver island films are outperformed by carbon dots, with a 96.3 fg/ml detection limit compared to 50 ng/ml [18,67]. However, it is not always the case that older methodologies are outperformed by newer ones. For example, the plasmonic chip prepared by Dr. Tawa in 2013 has a significantly lower LOD of 700 fM for the detection of epidermal growth factor receptor, compared to the aptamer modified AgNPs from 2016, which produced an LOD of 625 pM for the detection of platelet-derived growth factor-BB [69,72]. Overall, it can be observed that more complex plasmonic nanostructures, metal composites, carbon dot and quantum dot complexes, multilayered plasmonic chips, etc. have increased the level of sensitivity for the detection of all analyte types.

It should be noted that the most popular substrate materials were undeniably silver and gold, as they are excellent plasmonic materials and precursors for the variety of surface enhancing nanostructures [20,23,24,71,79,81,89]. However, the choice between the two of them can be difficult, as each of them has their advantages and disadvantages. In particular, silver is the first plasmonic material that was used for SEF, due to its high theoretical enhancement and relative abundance compared to gold [9,27]. On the other hand, silver nanostructures are more prone to oxidation in comparison with gold, especially in concentrated salt solutions and even in atmospheric conditions [102,103]. This makes gold nanostructures more suitable substrates in the majority of cases. However, the cost-efficiency of silver nanostructures is a lot more attractive compared to that of gold. Despite this, the applicability of both metals is limited due to the contamination by S-containing and C-containing compounds [104,105]. This disadvantage opens an opportunity for the development of non-noble nanostructures, like Al and Si, which are more robust and cost-efficient [101,106]. One such fresh example is shown by our research group, in which we applied organic carbon dots for bacteria labeling on Al foil and Al film substrates [107]. The results showed a high level of contrast and fluorescence enhancement on Al substrates, which was comparable or even better than the Au film.

Table 5
Applications of SEF classified by substrate.

Substrate	[Ref, Year] Enhancement factor
Ag film, Av EF = 20.1	[16,1997] 14; [47,2007] 7; [52,2009] 2–6.4; [18,2005] 10–15; [79,2007] 9; [17,2001] 15–2000; [87,2010] 10–20; [95,2012] 200–400
AgNPs and modifications, Av EF = 14.5	[36,2014] 5; [42,2014] 9; [45,2013] 50; [51,2014] 10.8; [78,2009] 11–37; [20,2011] 36–126; [79,2012] >25; [21,2013] 2.4; [53,2012] 4;
Ag core shell NPs; Av EF =6.5	[35,2014] 2.5; [19,2010] 1.3; [46,2007] 20; [48,2014] 32; [14,2004] 3–5; [65,2014] 6.4; [71,2005] 10.8; [76,1998] 20; [43,2015] 4; [63,2013] 3;
Ag nanostructures, Av EF =41 or AvEF =14 (without outlier ref. 97)	[44,2017] 100; [90,2016] 28; [91,2017] 42; [92,2017] 10; [97,2014] $0.5 \pm 0.1 \times 10^5$ $1.4 \pm 0.6 \times 10^5$; [98,2009] >15; [37,2016] 3;
AuNPs and modifications Av EF =16	[34,2007] 1100; [39,2008] 5; [74] 2; [41,2014] 6;
Au nanostructures; Av EF =56.2	[44,2013] 1100; [62,2013] 50; [84,2000] 14.2; [94,2018] 2; [96,2014] 2.3–35; [98,2009] >15; [60,2012] 8460 (for 100 nM IgG)
CDs; Av EF =31.0	[67,2017] 17.2; [100,2017] 50; [107,2020] 35
QDs; Av EF =29.3	[31,2014] 9; [91,2017] 42; [101,2020] 450–480; [22,2014] 2–9;
Miscellaneous; (Plasmonic chip and AlNPs) Av EF $=2 \times 10^3$	[69,2013] 300; [52,2009] 200–3500;

Av EF is the logarithmic average of enhancement factors.

7.1. Impact of the substrate on SEF enhancement

We can make several conclusions from Table 5 below about how enhancement in SEF is related to substrate morphology and composition.

If we exclude just two miscellaneous substrates, as a category with the highest average EFs (500), all other kinds of substrates demonstrate average EF's within one order of magnitude. These average EFs range from 6.5 for Ag core-shell nanoparticles and 15 for other silver nanoparticles to ~30 for Carbon and Quantum Dots and up to 14 for gold nanostructures, if we exclude EF = 10^5 from the Todescato et al. publication as an impressive positive outlier. If we keep the Ag-FON substrate in the calculated average, the winners by EFs would be substrates made of silver nanostructures, with an average logarithmic EF of 41. Todescato et al. publication reported the highest enhancement factor known to date, of 140,000 for MEF of SEF. His group employed the well-known silver film over nanosphere (Ag–FON) plasmonic substrates, described by Van Duyne et al. in 1993 and used to achieve high and relatively reproducible enhancement for SERS [108]. This substrate was fabricated by a deposition of up to a 150 nm layer of silver onto the mask, prepared from a monolayer of polystyrene beads (150 nm diameter), and used for detection of Ochratoxin A in food and drinks. This procedure was presented and discussed in more detail and with some additions in Greeneltch et al. [109]. Overall, it is a bit surprising that we found no other application of Ag-FON or Au-FON reported in SEF literature. This substrate should have great untapped potential for SEF applications in biodetection. The second-best substrate in terms of analytical EF was reported by Stephen Y. Chou's research group for Disk-coupled dots-on-pillar antenna array (D2PA). It produced an EF of 8460 for the detection of a 100 nM fluorescent-labeled IgG concentration. This array made from gold nanostructures was already shown in Fig. 5. The fabrication of this D2PA substrate appears to be a bit more complicated than the fabrication of Ag-FON substrate, but fluorescence enhancement of Single-Molecule Fluorophore, with up to a 4×10^6 fold EF at Hot Spot was reported for the former substrate, which is probably the highest hot spot SEF EF that we have found in literature. The publication of the Geddes group about SEF on aluminum nanoparticles demonstrated that not only silver and gold can produce relatively high EFs [51]. They showed that SEF on an array of aluminum nanoparticles can produce an enhancement in the 200–3500 range, depending on analyte molecule orientation. Aluminum may be used as a promising SEF material, capable of achieving high enhancement sometimes on par with gold, as was demonstrated in SEF of core-shell QDs in bacterial cells on the surface of Al foil and Al film, where EF's of up to 480 were obtained.

8. Conclusion

Overall, reproducible nanofabricated structures made from silver and gold with controlled morphology and reproducible gaps, like those fabricated by Ag-FON and D2PA methods, show probably the greatest promise in the application of SEF for biosensing and biodetection. Another noticeable trend is an increase in applications of quantum and carbon Nanodots for Surface-Enhanced fluorescence. Overall, more complex plasmonic nanostructures, metal composites, carbon dot, and quantum dot complexes, multilayered plasmonic chips, etc., are moving forward the level of sensitivity in the detection of all analyte types.

In conclusion, with this mini-review, we have presented and discussed a substantial amount of studies regarding the use of the SEF phenomenon. We categorized these studies into several sections according to the nature of the analyte and its complexity. In each section, we adhered to the chronological ordering of articles and summed up the information in the form of tables. We concentrated our attention on the quantitative aspect of each study, as hard data is the most representative evidence of successful application. Overall, we believe that this mini-review can provide insight into the history, current state, and possible future directions of this research area.

Funding

This review is supported by the Nazarbayev University Faculty Development Competitive Research grant 090118FD5352 (Kazakhstan) "Fundamental and applied SERS for detection of cancer biomarkers" (FASERSDCB).

Author contributions

Alisher Sultangaziyev is responsible for Writing - original draft and Writing - review & editing. Rostislav Bukasov is responsible for Conceptualization, Funding acquisition, Writing - review & editing.

Declaration of Competing Interest

The authors declare that there is no conflict of interest regarding the publication of this paper.

Acknowledgment

Yunona Bukasova is acknowledged for proofreading of the manuscript.

References

[1] H.S. Rye, J.M. Dabora, M.A. Quesada, R.A. Mathies, A.N. Glazer, Fluorometric assay using dimeric dyes for double- and single-stranded DNA and RNA with Picogram sensitivity, Anal. Biochem. 208 (1) (1993) 144–150.
[2] A. Jablonski, Efficiency of anti-stokes fluorescence in dyes, Nature 131 (3319) (1933) 839–840.
[3] S.J. Strickler, R.A. Berg, Relationship between absorption intensity and fluorescence lifetime of molecules, J. Chem. Phys. 37 (4) (1962) 814–822.
[4] G.W. Ford, W.H. Weber, Electromagnetic interactions of molecules with metal surfaces, Phys. Rep. 113 (4) (1984) 195–287.
[5] R.R. Chance, A.H. Miller, A. Prock, R. Silbey, Fluorescence and energy transfer near interfaces: the complete and quantitative description of the Eu+3/mirror systems, J. Chem. Phys. 63 (4) (1975) 1589–1595.
[6] M. Moskovits, Surface-enhanced spectroscopy, Rev. Mod. Phys. 57 (3) (1985) 783–826.
[7] J.R. Lakowicz, Radiative decay engineering 5: metal-enhanced fluorescence and plasmon emission, Anal. Biochem. 337 (2) (2005) 171–194.
[8] A. Wokaun, Surface-enhanced electromagnetic processes, in: H. Ehrenreich, D. Turnbull, F. Seitz (Eds.), Solid State Physics, Academic Press, 1984, pp. 223–294.
[9] C.D. Geddes, H. Cao, I. Gryczynski, Z. Gryczynski, J. Fang, J.R. Lakowicz, Metal-enhanced fluorescence (MEF) due to silver colloids on a planar surface: potential applications of Indocyanine green to in vivo imaging, J. Phys. Chem. A 107 (18) (2003) 3443–3449.
[10] K.H. Drexhage, H. Kuhn, F.P. Schäfer, Variation of the fluorescence decay time of a molecule in front of a mirror, Ber. Bunsenges. Phys. Chem. 72 (2) (1968) 329.
[11] K.H. Drexhage, Influence of a dielectric interface on fluorescence decay time, J. Lumin. 1-2 (1970) 693–701.
[12] J.R. Lakowicz, Radiative decay engineering: biophysical and biomedical applications, Anal. Biochem. 298 (1) (2001) 1–24.
[13] D.G. Chris, G. Ignacy, M. Joanna, G. Zygmunt, R.L. Joseph, Metal-enhanced fluorescence: potential applications in HTS, Comb. Chem. High Throughput Screen. 6 (2) (2003) 109–117.
[14] K. Aslan, J.R. Lakowicz, H. Szmacinski, C.D. Geddes, Metal-enhanced fluorescence solution-based sensing platform, J. Fluoresc. 14 (6) (2004) 677–679.
[15] K. Aslan, I. Gryczynski, J. Malicka, E. Matveeva, J.R. Lakowicz, C.D. Geddes, Metal-enhanced fluorescence: an emerging tool in biotechnology, Curr. Opin. Biotechnol. 16 (1) (2005) 55–62.
[16] T. Schalkhammer, F. Aussenegg, A. Leitner, H. Brunner, G. Hawa, C. Lobmaier, F. Pittner, Detection of fluorophore-labeled antibodies by surface-enhanced fluorescence on metal nanoislands, SPIE 2976 (1997) 129–136.
[17] J.R. Lakowicz, B. Shen, Z. Gryczynski, S. D'Auria, I. Gryczynski, Intrinsic fluorescence from DNA can be enhanced by metallic particles, Biochem. Biophys. Res. Commun. 286 (5) (2001) 875–879.
[18] E.G. Matveeva, Z. Gryczynski, J.R. Lakowicz, Myoglobin immunoassay based on metal particle-enhanced fluorescence, J. Immunol. Methods 302 (1) (2005) 26–35.
[19] F. Tang, F. He, H. Cheng, L. Li, Self-assembly of conjugated polymer-Ag@SiO2 hybrid fluorescent nanoparticles for application to cellular imaging, Langmuir 26 (14) (2010) 11774–11778.
[20] H. Li, W. Qiang, M. Vuki, D. Xu, H.-Y. Chen, Fluorescence enhancement of silver nanoparticle hybrid probes and ultrasensitive detection of IgE, Anal. Chem. 83 (23) (2011) 8945–8952.

[21] W. Qiang, H. Li, D. Xu, Metal enhanced fluorescent biosensing assays for DNA through the coupling of silver nanoparticles, Anal. Methods 5 (3) (2013) 629–635.
[22] S.R. Ahmed, M.A. Hossain, J.Y. Park, S.-H. Kim, D. Lee, T. Suzuki, J. Lee, E. Y. Park, Metal enhanced fluorescence on nanoporous gold leaf-based assay platform for virus detection, Biosens. Bioelectron. 58 (2014) 33–39.
[23] Z. Mei, L. Tang, Surface-plasmon-coupled fluorescence enhancement based on ordered gold nanorod array biochip for ultrasensitive DNA analysis, Anal. Chem. (Washington, DC, U. S.) 89 (1) (2017) 633–639.
[24] T. Tian, Y. Zhong, C. Deng, H. Wang, Y. He, Y. Ge, G. Song, Brightly near-infrared to blue emission tunable silver-carbon dot nanohybrid for sensing of ascorbic acid and construction of logic gate, Talanta 162 (2017) 135–142.
[25] W. Deng, F. Xie, H.T.M.C.M. Baltar, E.M. Goldys, Metal-enhanced fluorescence in the life sciences: here, now and beyond, Phys. Chem. Chem. Phys. 15 (38) (2013) 15695–15708.
[26] J.R. Lakowicz, C.D. Geddes, I. Gryczynski, J. Malicka, Z. Gryczynski, K. Aslan, J. Lukomska, E. Matveeva, J. Zhang, R. Badugu, J. Huang, Advances in surface-enhanced fluorescence, J. Fluoresc. 14 (4) (2004) 425–441.
[27] K. Aslan, J.R. Lakowicz, C.D. Geddes, Metal-enhanced fluorescence using anisotropic silver nanostructures: critical progress to date, Anal. Bioanal. Chem. 382 (4) (2005) 926–933.
[28] D. Darvill, A. Centeno, F. Xie, Plasmonic fluorescence enhancement by metal nanostructures: shaping the future of bionanotechnology, Phys. Chem. Chem. Phys. 15 (38) (2013) 15709–15726.
[29] Y. Jeong, Y.-M. Kook, K. Lee, W.-G. Koh, Metal enhanced fluorescence (MEF) for biosensors: general approaches and a review of recent developments, Biosens. Bioelectron. 111 (2018) 102–116.
[30] E. Fort, S. Grésillon, Surface enhanced fluorescence, J. Phys. D. Appl. Phys. 41 (1) (2007) 013001.
[31] P.J.G. Goulet, R.F. Aroca, Surface-enhancement of fluorescence near noble metal nanostructures, in: C.D. Geddes, J.R. Lakowicz (Eds.), Radiative Decay Engineering, Springer US, Boston, MA, 2005, pp. 223–247.
[32] M. Bauch, K. Toma, M. Toma, Q. Zhang, J. Dostalek, Plasmon-enhanced fluorescence biosensors: a review, Plasmonics 9 (4) (2014) 781–799.
[33] D.V. Guzatov, S.V. Vaschenko, V.V. Stankevich, A.Y. Lunevich, Y.F. Glukhov, S. V. Gaponenko, Plasmonic enhancement of molecular fluorescence near silver nanoparticles: theory, modeling, and experiment, J. Phys. Chem. C 116 (19) (2012) 10723–10733.
[34] G.K. Darbha, A. Ray, P.C. Ray, Gold nanoparticle-based miniaturized nanomaterial surface energy transfer probe for rapid and ultrasensitive detection of mercury in soil, water, and fish, ACS Nano 1 (3) (2007) 208–214.
[35] N. Sui, L. Wang, T. Yan, F. Liu, J. Sui, Y. Jiang, J. Wan, M. Liu, W.W. Yu, Selective and sensitive biosensors based on metal-enhanced fluorescence, Sensors Actuators B Chem. 202 (2014) 1148–1153.
[36] Z. Zhou, H. Huang, Y. Chen, F. Liu, C.Z. Huang, N. Li, A distance-dependent metal-enhanced fluorescence sensing platform based on molecular beacon design, Biosens. Bioelectron. 52 (2014) 367–373.
[37] B. Sun, C. Wang, S. Han, Y. Hu, L. Zhang, Metal-enhanced fluorescence-based multilayer core–shell Ag-nanocube@SiO2@PMOs nanocomposite sensor for Cu2 + detection, RSC Adv. 6 (66) (2016) 61109–61118.
[38] L. Liang, F. Lan, S. Ge, J. Yu, N. Ren, M. Yan, Metal-enhanced ratiometric fluorescence/naked eye bimodal biosensor for lead ions analysis with bifunctional nanocomposite probes, Anal. Chem. 89 (6) (2017) 3597–3605.
[39] S.S.R. Dasary, U.S. Rai, H. Yu, Y. Anjaneyulu, M. Dubey, P.C. Ray, Gold nanoparticle based surface enhanced fluorescence for detection of organophosphorus agents, Chem. Phys. Lett. 460 (1) (2008) 187–190.
[40] Y. Wang, Z. Li, H. Li, M. Vuki, D. Xu, H.Y. Chen, A novel aptasensor based on silver nanoparticle enhanced fluorescence, Biosens. Bioelectron. 32 (1) (2012) 76–81.
[41] Y. Zhang, T. Hei, Y. Cai, Q. Gao, Q. Zhang, Affinity binding-guided fluorescent nanobiosensor for acetylcholinesterase inhibitors via distance modulation between the fluorophore and metallic nanoparticle, Anal. Chem. 84 (6) (2012) 2830–2836.
[42] Y. Tang, Q. Yang, T. Wu, L. Liu, Y. Ding, B. Yu, Fluorescence enhancement of cadmium Selenide quantum dots assembled on silver nanoparticles and its application to glucose detection, Langmuir 30 (22) (2014) 6324–6330.
[43] E. Jang, M. Kim, W.-G. Koh, Ag@SiO2-entrapped hydrogel microarray: a new platform for a metal-enhanced fluorescence-based protein assay, Analyst 140 (10) (2015) 3375–3383.
[44] R. Rajamanikandan, M. Ilanchelian, Highly selective and sensitive biosensing of dopamine based on glutathione coated silver nanoclusters enhanced fluorescence, New J. Chem. 41 (24) (2017) 15244–15250.
[45] Q. Cheng, Y. He, Y. Ge, J. Zhou, G. Song, Ultrasensitive detection of heparin by exploiting the silver nanoparticle-enhanced fluorescence of graphitic carbon nitride (g-C3N4) quantum dots, Microchim. Acta 185 (7) (2018).
[46] K. Aslan, M. Wu, J.R. Lakowicz, C.D. Geddes, Metal enhanced fluorescence solution-based sensing platform 2: fluorescent core-shell Ag@SiO2 nanoballs, J. Fluoresc. 17 (2) (2007) 127–131.
[47] K. Ray, R. Badugu, J.R. Lakowicz, Sulforhodamine adsorbed Langmuir−Blodgett layers on silver island films: effect of probe distance on the metal-enhanced fluorescence, J. Phys. Chem. C 111 (19) (2007) 7091–7097.
[48] L. Lu, Y. Qian, L. Wang, K. Ma, Y. Zhang, Metal-enhanced fluorescence-based core–shell Ag@SiO2 nanoflares for affinity biosensing via target-induced structure switching of aptamer, ACS Appl. Mater. Interfaces 6 (3) (2014) 1944–1950.
[49] K. Wang, J. Liao, X. Yang, M. Zhao, M. Chen, W. Yao, W. Tan, X. Lan, A label-free aptasensor for highly sensitive detection of ATP and thrombin based on metal-enhanced PicoGreen fluorescence, Biosens. Bioelectron. 63 (2015) 172–177.
[50] Q. Song, M. Peng, L. Wang, D. He, J. Ouyang, A fluorescent aptasensor for amplified label-free detection of adenosine triphosphate based on core-shell Ag@SiO2 nanoparticles, Biosens. Bioelectron. 77 (2016) 237–241.
[51] M.H. Chowdhury, K. Ray, S.K. Gray, J. Pond, J.R. Lakowicz, Aluminum nanoparticles as substrates for metal-enhanced fluorescence in the ultraviolet for the label-free detection of biomolecules, Anal. Chem. 81 (4) (2009) 1397–1403.
[52] H. Szmacinski, K. Ray, J.R. Lakowicz, Metal-enhanced fluorescence of tryptophan residues in proteins: application toward label-free bioassays, Anal. Biochem. 385 (2) (2009) 358–364.
[53] H. Tan, Y. Chen, Silver nanoparticle enhanced fluorescence of europium (III) for detection of tetracycline in milk, Sensors Actuators B Chem. 173 (2012) 262–267.
[54] X. Yang, S. Zhu, Y. Dou, Y. Zhuo, Y. Luo, Y. Feng, Novel and remarkable enhanced-fluorescence system based on gold nanoclusters for detection of tetracycline, Talanta 122 (2014) 36–42.
[55] S.N. Yin, T. Yao, T.H. Wu, Y. Zhang, P. Wang, Novel metal nanoparticle-enhanced fluorescence for determination of trace amounts of fluoroquinolone in aqueous solutions, Talanta 174 (2017) 14–20.
[56] B. Tan, D. Wang, Z. Cai, X. Quan, H. Zhao, Extending suitability of physisorption strategy in fluorescent platforms design: surface passivation and covalent linkage on MOF nanosheets with enhanced OTC detection sensitivity, Sensors Actuators B Chem. 303 (2020) 127230.
[57] L. Yu, H. Chen, J. Yue, X. Chen, M. Sun, J. Hou, K.A. Alamry, H.M. Marwani, X. Wang, S. Wang, Europium metal-organic framework for selective and sensitive detection of doxycycline based on fluorescence enhancement, Talanta 207 (2020) 120297.
[58] M.H. Chowdhury, K. Ray, K. Aslan, J.R. Lakowicz, C.D. Geddes, Metal-enhanced fluorescence of Phycobiliproteins from heterogeneous plasmonic nanostructures, J. Phys. Chem. C 111 (51) (2007) 18856–18863.
[59] K. Aslan, T.A.J. Grell, Rapid and sensitive detection of troponin I in human whole blood samples by using silver nanoparticle films and microwave heating, Clin. Chem. 57 (5) (2011) 746–752.
[60] C.-H. Chao, Y.-F. Chang, H.-C. Chen, L.-Y. Lin, P.-C. Yu, Y.-S. Chang, Y.-J. Lee, C. Chou, Detection of urine cofilin-1 from patients hospitalized in the intensive care unit using the metal-enhanced fluorescence technique, Sensors Actuators B Chem. 173 (2012) 184–190.
[61] D. Punj, M. Mivelle, S.B. Moparthi, T.S. van Zanten, H. Rigneault, N.F. van Hulst, M.F. Garcia-Parajo, J. Wenger, A plasmonic "antenna-in-box" platform for enhanced single-molecule analysis at micromolar concentrations, Nat. Nanotechnol. 8 (7) (2013) 512–516.
[62] K. Ray, J.R. Lakowicz, Metal-enhanced fluorescence lifetime imaging and spectroscopy on a modified SERS substrate, J. Phys. Chem. C 117 (30) (2013) 15790–15797.
[63] P.P. Hu, L.L. Zheng, L. Zhan, J.Y. Li, S.J. Zhen, H. Liu, L.F. Luo, G.F. Xiao, C. Z. Huang, Metal-enhanced fluorescence of nano-core–shell structure used for sensitive detection of prion protein with a dual-aptamer strategy, Anal. Chim. Acta 787 (2013) 239–245.
[64] M. Tsuneyasu, C. Sasakawa, N. Naruishi, Y. Tanaka, Y. Yoshida, K. Tawa, Sensitive detection of interleukin-6 on a plasmonic chip by grating-coupled surface-plasmon-field-enhanced fluorescence imaging, Jpn. J. Appl. Phys. 53 (6S) (2014) 5, 06JL05/1-06JL05/5.
[65] Y. Pang, Z. Rong, J. Wang, R. Xiao, S. Wang, A fluorescent aptasensor for H5N1 influenza virus detection based-on the core–shell nanoparticles metal-enhanced fluorescence (MEF), Biosens. Bioelectron. 66 (2015) 527–532.
[66] Z. Chen, H. Li, W. Jia, X. Liu, Z. Li, F. Wen, N. Zheng, J. Jiang, D. Xu, Bivalent aptasensor based on silver-enhanced fluorescence polarization for rapid detection of lactoferrin in milk, Anal. Chem. 89 (11) (2017) 5900–5908.
[67] D.-D. Xu, C. Liu, C.-Y. Li, C.-Y. Song, Y.-F. Kang, C.-B. Qi, Y. Lin, D.-W. Pang, H.-W. Tang, Dual amplification fluorescence assay for alpha Fetal protein utilizing Immunohybridization chain reaction and metal-enhanced fluorescence of carbon nanodots, ACS Appl. Mater. Interfaces 9 (43) (2017) 37606–37614.
[68] N.M. Noah, S. Alam, O.A. Sadik, Detection of inducible nitric oxide synthase using a suite of electrochemical, fluorescence, and surface plasmon resonance biosensors, Anal. Biochem. 413 (2) (2011) 157–163.
[69] K. Tawa, M. Umetsu, H. Nakazawa, T. Hattori, I. Kumagai, Application of 300× enhanced fluorescence on a Plasmonic Chip modified with a Bispecific antibody to a sensitive Immunosensor, ACS Appl. Mater. Interfaces 5 (17) (2013) 8628–8632.
[70] D. Zhu, W. Li, H.M. Wen, S. Yu, Z.Y. Miao, A. Kang, A. Zhang, Silver nanoparticles-enhanced time-resolved fluorescence sensor for VEGF165 based on Mn-doped ZnS quantum dots, Biosens. Bioelectron. 74 (2015) 1053–1060.
[71] H. Li, M. Wang, W. Qiang, H. Hu, W. Li, D. Xu, Metal-enhanced fluorescent detection for protein microarrays based on a silver plasmonic substrate, Anal. (Cambridge, U. K.) 139 (7) (2014) 1653–1660.
[72] Y. Wang, H. Li, D. Xu, Aptamers-based sandwich assay for silver-enhanced fluorescence multiplex detection, Anal. Chim. Acta 905 (2016) 149–155.
[73] M.M.L.M. Vareiro, J. Liu, W. Knoll, K. Zak, D. Williams, A.T.A. Jenkins, Surface plasmon fluorescence measurements of human chorionic gonadotrophin: role of antibody orientation in obtaining enhanced sensitivity and limit of detection, Anal. Chem. 77 (8) (2005) 2426–2431.
[74] P. Yager, T. Edwards, E. Fu, K. Helton, K. Nelson, M.R. Tam, B.H. Weigl, Microfluidic diagnostic technologies for global public health, Nature 442 (7101) (2006) 412–418.

[75] D.A. Giljohann, C.A. Mirkin, Drivers of biodiagnostic development, Nature 462 (7272) (2009) 461–464.
[76] K. Sokolov, G. Chumanov, T.M. Cotton, Enhancement of molecular fluorescence near the surface of colloidal metal films, Anal. Chem. 70 (18) (1998) 3898–3905.
[77] Y. Wang, A. Brunsen, U. Jonas, J. Dostálek, W. Knoll, Prostate specific antigen biosensor based on long range surface plasmon-enhanced fluorescence spectroscopy and dextran hydrogel binding matrix, Anal. Chem. 81 (23) (2009) 9625–9632.
[78] R. Nooney, A. Clifford, X. LeGuevel, O. Stranik, C. McDonagh, B.D. MacCraith, Enhancing the analytical performance of immunoassays that employ metal-enhanced fluorescence, Anal. Bioanal. Chem. 396 (3) (2010) 1127–1134.
[79] H. Li, C.-Y. Chen, X. Wei, W. Qiang, Z. Li, Q. Cheng, D. Xu, Highly sensitive detection of proteins based on metal-enhanced fluorescence with novel silver nanostructures, Anal. Chem. 84 (20) (2012) 8656–8662.
[80] L. Zhou, F. Ding, H. Chen, W. Ding, W. Zhang, S.Y. Chou, Enhancement of Immunoassay's fluorescence and detection sensitivity using three-dimensional plasmonic nano-antenna-dots Array, Anal. Chem. 84 (10) (2012) 4489–4495.
[81] X. Yang, Y. Zhuo, S. Zhu, Y. Luo, Y. Feng, Y. Xu, Selectively assaying CEA based on a creative strategy of gold nanoparticles enhancing silver nanoclusters' fluorescence, Biosens. Bioelectron. 64 (2015) 345–351.
[82] D.-D. Xu, Y.-L. Deng, C.-Y. Li, Y. Lin, H.-W. Tang, Metal-enhanced fluorescent dye-doped silica nanoparticles and magnetic separation: a sensitive platform for one-step fluorescence detection of prostate specific antigen, Biosens. Bioelectron. 87 (2017) 881–887.
[83] B. Della Ventura, M. Gelzo, E. Battista, A. Alabastri, A. Schirato, G. Castaldo, G. Corso, F. Gentile, R. Velotta, Biosensor for point-of-care analysis of immunoglobulins in urine by metal enhanced fluorescence from gold nanoparticles, ACS Appl. Mater. Interfaces 11 (4) (2019) 3753–3762.
[84] T. Liebermann, W. Knoll, P. Sluka, R. Herrmann, Complement hybridization from solution to surface-attached probe-oligonucleotides observed by surface-plasmon-field-enhanced fluorescence spectroscopy, Colloids Surf. A Physicochem. Eng. Asp. 169 (1) (2000) 337–350.
[85] K. Aslan, J. Huang, G.M. Wilson, C.D. Geddes, Metal-enhanced fluorescence-based RNA sensing, J. Am. Chem. Soc. 128 (13) (2006) 4206–4207.
[86] K. Aslan, Y. Zhang, S. Hibbs, L. Baillie, M.J.R. Previte, C.D. Geddes, Microwave-accelerated metal-enhanced fluorescence: application to detection of genomic and exosporium anthrax DNA in <30 seconds, Analyst 132 (11) (2007) 1130–1138.
[87] L. Touahir, E. Galopin, R. Boukherroub, A.C. Gouget-Laemmel, J.-N. Chazalviel, F. Ozanam, S. Szunerits, Localized surface plasmon-enhanced fluorescence spectroscopy for highly-sensitive real-time detection of DNA hybridization, Biosens. Bioelectron. 25 (12) (2010) 2579–2585.
[88] J. Chen, Q. Chen, C. Gao, M. Zhang, B. Qin, H. Qiu, A SiO2 NP–DNA/silver nanocluster sandwich structure-enhanced fluorescence polarization biosensor for amplified detection of hepatitis B virus DNA, J. Mater. Chem. B 3 (6) (2015) 964–967.
[89] G.M. Santos, F. Zhao, J. Zeng, M. Li, W.-C. Shih, Label-free, zeptomole cancer biomarker detection by surface-enhanced fluorescence on nanoporous gold disk plasmonic nanoparticles, J. Biophotonics 8 (10) (2015) 855–863.
[90] X. Ji, C. Xiao, W.-F. Lau, J. Li, J. Fu, Metal enhanced fluorescence improved protein and DNA detection by zigzag Ag nanorod arrays, Biosens. Bioelectron. 82 (2016) 240–247.
[91] A. Kannegulla, Y. Liu, B. Wu, L.-J. Cheng, Plasmonic open-ring nanoarrays for broadband fluorescence enhancement and ultrasensitive DNA detection, J. Phys. Chem. C 122 (1) (2018) 770–776.
[92] Q. Wei, G. Acuna, S. Kim, C. Vietz, D. Tseng, J. Chae, D. Shir, W. Luo, P. Tinnefeld, A. Ozcan, Plasmonics enhanced smartphone fluorescence microscopy, Sci. Rep. 7 (1) (2017) 2124.
[93] L. Liang, F. Lan, X. Yin, S. Ge, J. Yu, M. Yan, Metal-enhanced fluorescence/visual bimodal platform for multiplexed ultrasensitive detection of microRNA with reusable paper analytical devices, Biosens. Bioelectron. 95 (2017) 181–188.
[94] J. Wang, Z. Jia, Metal nanoparticles/porous silicon microcavity enhanced surface plasmon resonance fluorescence for the detection of DNA, Sensors 18 (2) (2018) 661/1–661/12.
[95] A.I. Dragan, M.T. Albrecht, R. Pavlovic, A.M. Keane-Myers, C.D. Geddes, Ultra-fast pg/ml anthrax toxin (protective antigen) detection assay based on microwave-accelerated metal-enhanced fluorescence, Anal. Biochem. 425 (1) (2012) 54–61.
[96] Y. Li, J. Sun, L. Wu, J. Ji, X. Sun, Y. Qian, Surface-enhanced fluorescence immunosensor using Au nano-crosses for the detection of microcystin-LR, Biosens. Bioelectron. 62 (2014) 255–260.
[97] F. Todescato, A. Antognoli, A. Meneghello, E. Cretaio, R. Signorini, R. Bozio, Sensitive detection of Ochratoxin A in food and drinks using metal-enhanced fluorescence, Biosens. Bioelectron. 57 (2014) 125–132.
[98] I. Abdulhalim, A. Karabchevsky, C. Patzig, B. Rauschenbach, B. Fuhrmann, E. Eltzov, R. Marks, J. Xu, F. Zhang, A. Lakhtakia, Surface-enhanced fluorescence from metal sculptured thin films with application to biosensing in water, Appl. Phys. Lett. 94 (6) (2009), 063106.
[99] C.-J. Huang, J. Dostalek, A. Sessitsch, W. Knoll, Long-range surface plasmon-enhanced fluorescence spectroscopy biosensor for ultrasensitive detection of *E. coli* O157:H7, Anal. Chem. 83 (3) (2011) 674–677.
[100] R. Bukasov, O. Filchakova, K. Gudun, M. Bouhrara, Strong surface enhanced florescence of carbon dot labeled bacteria cells observed with high contrast on gold film, J. Fluoresc. 28 (1) (2018) 1–4.
[101] A. Sultangaziyev, A. Akhmetova, Z. Kunushpayeva, A. Rapikov, O. Filchakova, R. Bukasov, Aluminum foil as a substrate for metal enhanced fluorescence of bacteria labelled with quantum dots, shows very large enhancement and high contrast, Sens. Bio-Sens. Res. 28 (2020) 100332.
[102] J.L. Elechiguerra, L. Larios-Lopez, C. Liu, D. Garcia-Gutierrez, A. Camacho-Bragado, M.J. Yacaman, Corrosion at the nanoscale: the case of silver nanowires and nanoparticles, Chem. Mater. 17 (24) (2005) 6042–6052.
[103] T.W.H. Oates, M. Losurdo, S. Noda, K. Hinrichs, The effect of atmospheric tarnishing on the optical and structural properties of silver nanoparticles, J. Phys. D. Appl. Phys. 46 (14) (2013) 145308.
[104] T. Ishida, S. Tsuneda, N. Nishida, M. Hara, H. Sasabe, W. Knoll, Surface-conditioning effect of gold substrates on octadecanethiol self-assembled monolayer growth, Langmuir 13 (17) (1997) 4638–4643.
[105] A. Matikainen, T. Nuutinen, T. Itkonen, S. Heinilehto, J. Puustinen, J. Hiltunen, J. Lappalainen, P. Karioja, P. Vahimaa, Atmospheric oxidation and carbon contamination of silver and its effect on surface-enhanced Raman spectroscopy (SERS), Sci. Rep. 6 (1) (2016) 37192.
[106] Z. Kunushpayeva, A. Rapikov, A. Akhmetova, A. Sultangaziyev, D. Dossym, R. Bukasov, Sandwich SERS immunoassay of human immunoglobulin on silicon wafer compared to traditional SERS substrate, gold film, Sens. Bio-Sens. Res. 29 (2020) 100355.
[107] R. Bukasov, Z. Kunushpayeva, A. Rapikov, S. Zhunussova, A. Sultangaziyev, O. Filchakova, High contrast surface enhanced fluorescence of carbon dot labeled bacteria cells on aluminum foil, J. Fluoresc. (2020), https://doi.org/10.1007/s10895-020-02610-2. In press.
[108] R.P.V. Duyne, J.C. Hulteen, D.A. Treichel, Atomic force microscopy and surface-enhanced Raman spectroscopy. I. Ag island films and Ag film over polymer nanosphere surfaces supported on glass, J. Chem. Phys. 99 (3) (1993) 2101–2115.
[109] N.G. Greeneltch, M.G. Blaber, A.-I. Henry, G.C. Schatz, R.P. Van Duyne, Immobilized Nanorod assemblies: fabrication and understanding of large area surface-enhanced Raman spectroscopy substrates, Anal. Chem. 85 (4) (2013) 2297–2303.